communications biology

A Nature Portfolio journal

Article

https://doi.org/10.1038/s42003-026-09776-8

Phasic and tonic arousal distinctly shape human decision bias

Stijn Adriaan Nuiten [1] ✉, Jan Willem De Gee [2,3], Jasper Brian Zantvoord [4,5], Philipp Sterzer [1], Johannes Jacobus Fahrenfort [6,7,8] & Simon van Gaal [3,8] ✉

Neuroscientific theories hypothesize that arousal fluctuations influence human perception and behavior in two functionally distinct ways: through variations in baseline state (tonic arousal) and by transient task-evoked bursts (phasic arousal). We combined causal (pharmacology) and correlational (pupillometry) methods to test the hypothesis that tonic and phasic arousal differentially influence decision biases in human male participants performing a yes/no visual detection task. Computational modeling of choice behavior and analyses of neural data (EEG) revealed that experimentally induced shifts in decision bias were associated with changes in preparatory activity over motor cortex resembling a starting-point bias in the decision formation. The behavioral, computational, and neural effects of strategic shifts in decision bias were weakest on trials with high phasic pupil-linked arousal, but did not relate to tonic pupil-linked arousal or pharmacology. In sharp contrast, tonic pupil-linked arousal and pharmacological interventions were associated with more liberal decision-making (increased proportion of "yes" choices) independent of task context. Thus, in line with the hypothesized functional distinction, tonic arousal was associated with inherent decision bias, whereas phasic arousal was related to context-dependent strategic shifts in decision bias.

Decision-making behavior is highly variable, even when identical evidence is repeatedly presented[1,2]. A substantial portion of this behavioral variability has been attributed to fluctuations in the arousal state of an organism, which influences attentional, sensory, and decision-making processes[3–5]. Fluctuations in arousal are primarily driven by the activity of catecholamines (i.e., dopamine and noradrenaline) and acetylcholine[4,6–8], although other neuromodulators (e.g., serotonin) contribute as well[9]. Seminal neurophysiological studies revealed that these neuromodulatory systems exhibit distinct dynamics that may serve unique functional purposes[10–14]. For example, tonic (i.e., baseline) activity of noradrenergic locus coeruleus (LC) neurons is non-monotonically related to sensory evoked potentials in rat barrel cortex[15], whereas phasic (i.e., transient bursting) activity in monkey LC has been observed in response to task-relevant cues and in close proximity to task-relevant responses[11,16], consistent with possible roles in decision-making and motor execution. Such functional distinctions between tonic and phasic neuromodulatory activity regimes form the basis of highly influential theories, such as the Adaptive Gain Theory[17].

In recent years, the functional distinction between tonic and phasic neuromodulator-driven arousal has been studied in humans via continuous measurements of pupil size, which—under equiluminance– correlate with (sub-)cortical activity of neuromodulators that drive arousal[18–20]. Tonic pupil-linked arousal is often calculated as the average pupil size in a baseline prestimulus window[21–24], whereas phasic arousal is usually calculated as the response-locked (baseline-corrected) task-evoked pupil response around the time of the behavioral response[18,25–27]. Converging evidence from human pupillometry studies indicates that inherent decision biases—i.e., not related to experimental manipulations—are weakest when phasic pupil-linked arousal is high (i.e., when the pupil is large during the response interval of the current or preceding trial)[18,25–30]. Moreover, experimentally induced or strategic decision biases, e.g., induced by changes in the proportion of trials containing a certain stimulus category, are also weakest when phasic pupil-linked arousal is high[26]. In contrast, tonic pupil-linked arousal does not seem to correlate with decision bias[18,26], but rather non-monotonically relates to perceptual sensitivity, with optimal performance at mid-level arousal[21–24,31].

[1]Department of Psychiatry (UPK), University of Basel, Basel, Switzerland. [2]Cognitive and Systems Neuroscience, Swammerdam Institute for Life Sciences, University of Amsterdam, Amsterdam, The Netherlands. [3]Amsterdam Brain & Cognition, University of Amsterdam, Amsterdam, The Netherlands. [4]Department of Psychiatry, Amsterdam UMC, Amsterdam, The Netherlands. [5]Amsterdam Neuroscience Research Institute, Amsterdam, The Netherlands. [6]Institute for Brain and Behavior Amsterdam, Vrije Universiteit Amsterdam, Amsterdam, The Netherlands. [7]Department of Experimental and Applied Psychology - Cognitive Psychology, Vrije Universiteit Amsterdam, Amsterdam, The Netherlands. [8]Department of Psychology, University of Amsterdam, Amsterdam, The Netherlands.
✉e-mail: stijnnuiten@gmail.com; simonvangaal@gmail.com

Despite this evidence for functionally distinct roles of tonic and phasic arousal in regulating human decision bias, three critical gaps in understanding remain. First, it is currently unknown which neural processes govern the relation between phasic (and possibly tonic) arousal and biased decision-making in human participants. Second, the claim that tonic arousal does not influence decision bias lacks sufficient empirical support. Some pharmacological studies have reported that causal elevations of tonic arousal do not affect inherent decision bias[23,32,33], but the lack of experimental control over decision biases in these studies limits definitive conclusions. Third, the respective contributions of the catecholaminergic and cholinergic systems remain unsolved, with prior work yielding partially conflicting accounts. One view holds that both systems attenuate top-down biases by amplifying bottom-up sensory drive[34–37]. In contrast, other work suggests a dissociation in their effects on cortical gain: catecholamines are thought to modulate response gain (steepening input-output functions), whereas acetylcholine is thought to modulate multiplicative gain (uniform scaling of outputs across inputs)[38]. Heightened response gain enhances the discriminability between noise and sensory signals, improving perceptual sensitivity, whereas increased multiplicative gain amplifies overall output levels—including noise-driven activity– potentially biasing responses toward signal presence.

The current study addressed these issues by combining correlational indices (pupillometry) and causal manipulations (pharmacology) of arousal in 28 human participants performing a challenging yes/no visual detection task in which decision bias was experimentally manipulated, while recording neural activity with electroencephalography (EEG). Decision bias was manipulated in two separate versions of the detection task, in which aversive buzzer tones were either presented following misses (i.e., target present, "no" response) to induce a liberal bias (saying "yes" more often) or following false alarms (i.e., target absent, "yes" response) to induce a conservative bias (saying "no" more often; similar to Kloosterman et al., 2019; Fig. 1C). Following a double-blind within-subject crossover design, atomoxetine (40 mg, ATX) was used to elevate tonic levels of catecholamines and donepezil (5 mg, DNP) was used to elevate tonic levels of acetylcholine, and these active drug conditions were compared to a placebo (PLC) control condition (Fig. 1A).

This study tested if and how inherent (task-independent) and strategic (task-related) decision biases were affected by pharmacological elevations of neuromodulatory drive and if they correlated with pupil-linked tonic and phasic arousal. Furthermore, EEG analyses and drift diffusion modeling (DDM) of choice behavior[39] were used to elucidate the neural and computational mechanisms possibly underlying arousal-driven modulations of decision bias. To anticipate the results, this study not only confirms the distinct functional roles of tonic and phasic arousal in shaping decision bias but also provides insights into the neural processes through which phasic arousal governs decision bias. Elevated tonic pupil-linked arousal was related to a lowered inherent decision criterion (i.e., more liberal decision-making), but exhibited no relation to task-dependent strategic shifts in decision bias. Pharmacological elevation of catecholamines (with ATX) and acetylcholine (with DNP) revealed a trend in the same direction. In sharp contrast, phasic pupil-linked arousal was selectively related to strategic shifts in decision bias, but did not correlate with inherent decision bias. Further neural and computational analyses suggested that the relation between phasic pupil-linked arousal and strategic decision bias could be attributed to modulations of anticipatory activity over motor cortex reflecting a "head start" (biased starting point) in the preparation of preferred behavioral responses. These findings illuminate the distinct mechanisms through

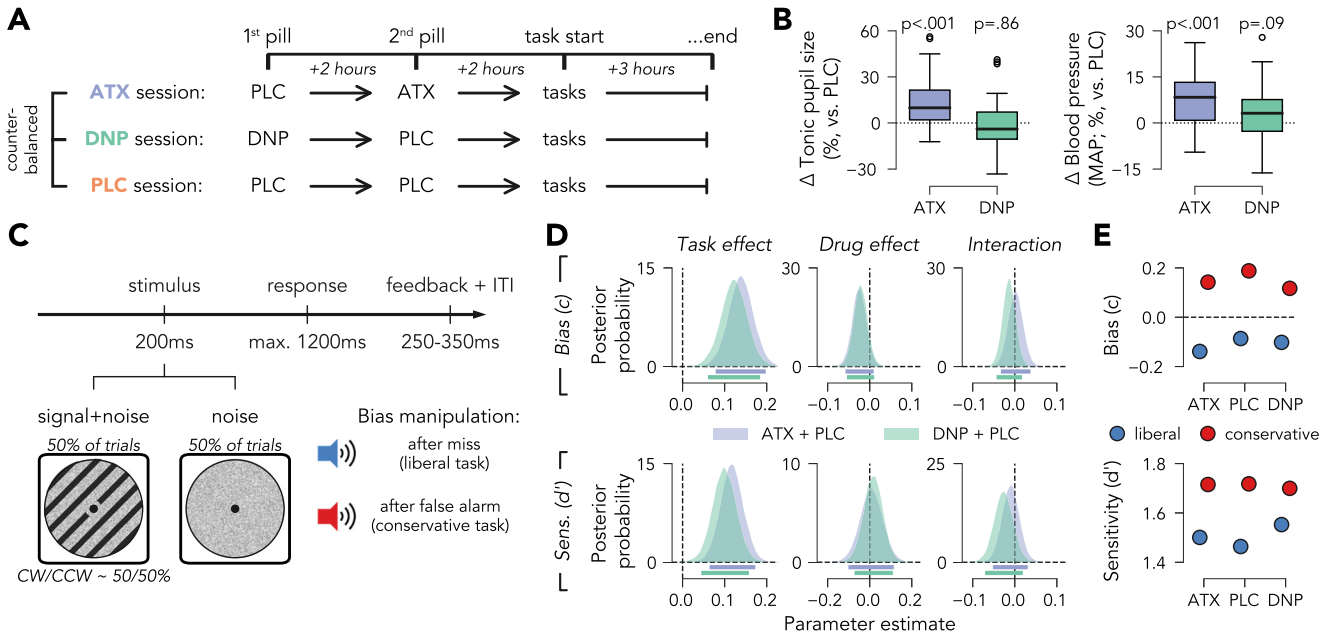

Fig. 1 | Experimental setup, pharmacology, and behavior. A Overview of drug intake and pharmacological sessions. Participants came to the lab on three occasions, on which they received either placebo (PLC), donepezil (DNP, 5 mg, data in green) or atomoxetine (ATX, 40 mg, data in blue). The drug order was counterbalanced across participants. **B** ATX, but not DNP, significantly increased physiological measures of arousal (MAP: mean arterial pressure). Error bars indicate the standard error of the mean across participants (SEM; $N = 28$). **C** Schematic representation of the visual yes/no detection task. Participants reported the presence (50% of trials) or absence (50% of trials) of Gabor patches that were presented centrally on top of patches containing dynamic noise. Gabor orientation (clockwise, CW; counter-clockwise, CCW) in target present trials was balanced, 50% of each orientation. Liberal task: an aversive tone was presented after misses (target present, "no" response). Conservative task: an aversive tone was presented after false alarms (target absent, "yes" response). **D** Decision bias (c) and perceptual sensitivity (d') were estimated by fitting hierarchical Bayesian probit regression models on single-trial data[40]. Two separate models were fit: the ATX-model was fit on data from the ATX and PLC sessions ("ATX + PLC", in blue), and the DNP-model was fit on data from the DNP and PLC sessions ("DNP + PLC", in green). Top row: posterior distributions for the effects of—from left to right– task, drug, and their interaction on criterion. Bottom row: same as top row, but for d'. Horizontal bars on the bottom of the plots demark the 95% credible interval ($CI_{95\%}$). **E** Estimates of criterion (top row) and d' (bottom row) derived from posterior distribution means for each drug condition and task.

which arousal shapes decision-making and offer a deeper understanding of the sources of variability in human behavior.

Results

Atomoxetine, but not donepezil, increases physiological measures of arousal

Several physiological measures of arousal were recorded at three moments during each session (see **Methods**). The measurements at the onset of the behavioral experiments were normalized (percentage) to the baseline measurement prior to ingestion of the first pill and were then compared between each drug condition (ATX, DNP) and placebo with a paired-sample *t* test and its Bayesian equivalent (note that for consistency, all Bayes Factors in the manuscript specify evidence in favor of the null-hypothesis, BF_{01}; see **Methods**). At the onset of the experiments (4 hours after ingestion of the first pill), ATX increased tonic pupil diameter ($t(27) = 4.03$, $p < 0.001$, $d = 1.08$, $BF_{01} = 0.01$; Fig. 1B—left panel) and mean arterial blood pressure ($t(27) = 4.33$, $p < 0.001$, $d = 0.97$, $BF_{01} = 6.50e^{-3}$; Fig. 1B—right panel), whereas DNP did not (tonic pupil diameter: $t(27) = 0.18$, $p = 0.86$, $d = 0.05$, $BF_{01} = 4.90$; mean arterial pressure: $t(27) = 1.76$, $p = 0.09$, $d = 0.45$, $BF_{01} = 1.29$; Fig. 1B). Thus, ATX, but not DNP, increased physiological measures of arousal.

Behavioral task alters decision bias and perceptual sensitivity, irrespective of drug condition

Participants performed two versions of a visual yes/no detection task in which they detected Gabor patches that were presented on top of dynamic visual noise (Fig. 1C). The only difference between the two task versions was a manipulation of decision bias through the presentation of non-monetary punishments (aversive sounds) following either miss trials (to induce a liberal decision bias; 'liberal task') or false alarm trials (to induce a conservative decision bias; 'conservative task').

Across drug conditions and tasks, participants were correct on 77.40% of all trials (s.d. ± 6.69%) and responded with a mean RT of 610 ms (s.d. ± 95 ms). As expected, presenting aversive sounds following specific errors resulted in strategic shifts in decision bias. In the liberal task (aversive sound after misses) versus conservative task (aversive sound after false alarms), miss rates were decreased and false alarm rates were increased (across drug conditions; miss rate: $t(27) = -3.28$, $p = .003$, $d = 0.63$, $BF_{01} = 0.07$; false alarm rate: $t(27) = 5.35$, $p < 0.001$, $d = 1.13$, $BF_{01} = 5.52e^{-4}$).

To more formally investigate the behavioral effects of the tasks and drug conditions, a hierarchical Bayesian probit regression model was fit to choice behavior data. This probit regression model is a generalized linear model (GLM) formulation of Signal Detection Theory (SDT), which allows to discern effects on perceptual sensitivity (d') and decision bias (criterion)[40,41]. The SDT-GLM model was further extended as a hierarchical Bayesian model. In hierarchical Bayesian models, single-subject parameter estimates are constrained by population-level distributions of that parameter, rendering parameter estimation more robust to outliers and low trial counts[42]. Two separate drug models were fitted: one model compared the effects of ATX with PLC ("ATX-model") and the other compared the effects of DNP with PLC ("DNP-model"). All regression models were effect-coded (see Methods), with the liberal task (and placebo) being coded as −1 and the conservative task (and ATX/DNP) as 1. Therefore, positive effects indicate that the dependent variable was increased for the conservative task (or ATX/DNP) over the liberal task (or PLC), and vice versa for negative effects. This modeling approach simultaneously facilitated estimating drug effects on inherent decision bias (i.e., main effect of drug on criterion) and drug effects on strategic shifts in decision bias (i.e., interaction effect between drug and task on criterion). A comparison with traditional SDT analyses is reported in Supplementary Fig. 1. For each Bayesian posterior distribution, the 95% credible interval ($CI_{95\%}$) and the probability of direction (pd) are reported[43,44]. The pd corresponds to the proportion of the posterior that lies on the same side of zero as the median estimate, providing a descriptive measure of how strongly the data support an effect in a particular direction. Importantly, and in contrast to a frequentist *p* value, pd does not evaluate compatibility with the null-hypothesis and is thus not used to make claims about significance. For visualisation purposes, group-level estimates of criterion and d' were reconstructed based on the median values of the posterior distributions for all experimental conditions (Fig. 1E).

Participants were well able to perform the detection task (d', ATX-model: pd > 0.999, $\mu = 1.60$, $\sigma = 0.09$, $CI_{95\%} = [1.42, 1.77]$; DNP-model: pd > 0.999, $\mu = 1.61$, $\sigma = 0.11$, $CI_{95\%} = [1.40, 1.81]$; Supplementary Fig. 2A) and exhibited no overall decision bias (criterion, ATX-model: pd = 0.82, $\mu = 0.03$, $\sigma = 0.03$, $CI_{95\%} = [-0.03, 0.08]$; DNP-model: pd = 0.84, $\mu = 0.03$, $\sigma = 0.03$, $CI_{95\%} = [-0.03, 0.09]$; Supplementary Fig. 2B). In both models, the conservative task increased criterion (ATX-model: pd > 0.999, $\mu = 0.14$, $\sigma = 0.03$, $CI_{95\%} = [0.08, 0.20]$; DNP-model: pd > 0.999, $\mu = 0.12$, $\sigma = 0.03$, $CI_{95\%} = [0.06, 0.18]$; Fig. 1D—upper left panel) and d' compared to the liberal task (ATX-model: pd > 0.999, $\mu = 0.12$, $\sigma = 0.03$, $CI_{95\%} = [0.06, 0.17]$; DNP-model: pd > 0.999, $\mu = 0.10$, $\sigma = 0.03$, $CI_{95\%} = [0.04, 0.16]$; Fig. 1D—lower left panel). The $CI_{95\%}$ for the drug effect on criterion overlapped with zero for both models, however, 93% (ATX-model) and 91% (DNP-model) of the posterior mass fell below zero, indicating a trend toward a reduction in inherent decision criterion (i.e., more liberal decision-making; ATX-model: pd = 0.93, $\mu = -0.03$, $\sigma = 0.02$, $CI_{95\%} = [-0.06, 0.01]$; DNP-model: pd = 0.91, $\mu = -0.02$, $\sigma = 0.02$, $CI_{95\%} = [-0.05, 0.01]$; Fig. 1D—upper middle panel). In contrast, there was no evidence for drug effects on d' (ATX-model: pd = 0.56, $\mu = 0.01$, $\sigma = 0.06$, $CI_{95\%} = [-0.10, 0.11]$; DNP-model: pd = 0.64, $\mu = 0.02$, $\sigma = 0.05$, $CI_{95\%} = [-0.07, 0.11]$; Fig. 1D—lower middle panel). Finally, there were no interactions between drug and the behavioral task, both in terms of criterion (ATX-model: pd = 0.54, $\mu = 0.00$, $\sigma = 0.02$, $CI_{95\%} = [-0.03, 0.04]$; DNP-model: pd = 0.83, $\mu = -0.01$, $\sigma = 0.02$, $CI_{95\%} = [-0.04, 0.02]$; Fig. 1D—upper right panel) and d' (ATX-model: pd = 0.69, $\mu = -0.01$, $\sigma = 0.02$, $CI_{95\%} = [-0.05, 0.03]$; DNP-model: pd = 0.88, $\mu = -0.03$, $\sigma = 0.02$, $CI_{95\%} = [-0.07, 0.02]$; Fig. 1D—lower right panel).

Thus, replicating earlier work, the behavioral task led to robust strategic shifts in decision bias and affected perceptual sensitivity[45]. Pharmacological elevation of tonic catecholaminergic and cholinergic levels revealed a trend toward more liberal decision-making behavior (i.e., more "yes" responses), but showed no evidence for changes in perceptual sensitivity or interactions with task context.

Tonic pupil-linked arousal related to inherent, but not strategic shifts in decision bias

The pharmacological intervention resulted in long-lasting elevations of neuromodulator levels, in the range of several hours (see Methods). In the absence of pharmacological interventions, neuromodulator levels, and hence tonic arousal, also fluctuate considerably over time and do so at different timescales, ranging from relatively durable changes in baseline neuromodulation (in the range of minutes and hours) to more transient, often task-evoked, neuromodulator activity (in the range of seconds). These fluctuations can be gauged by measuring pupil diameter under equiluminance[18–20]. Because the detection task was one of four experiments completed by the participants during each drug session (see Methods), trial durations and inter-trial intervals were relatively short to ensure that enough trials could be collected for each experiment. Although pupillometry experiments are usually more slow-paced (to reduce, but not eliminate, carryover effects in the pupil response from the preceding trial onto the current trial[46]), phasic pupil dynamics are not as sluggish as sometimes believed. For instance, pupil dilation following attentional orienting peaks after 500 ms[47,48] and pupil responses have even been shown to track attentional blinks during rapid stream visual presentation (RSVP) tasks with stimuli presented at 10 Hz[49,50]. Therefore, phasic pupil-linked arousal dynamics can even be studied in more rapid task designs, such as employed in the current study.

To demonstrate the variability in pupil-linked arousal over time, Fig. 2A shows a 200 s example trace of pupil size expressed as the percentage of the median pupil size during the experimental block. As can be seen, there are large fluctuations in pupil size (ranging from ~40% to

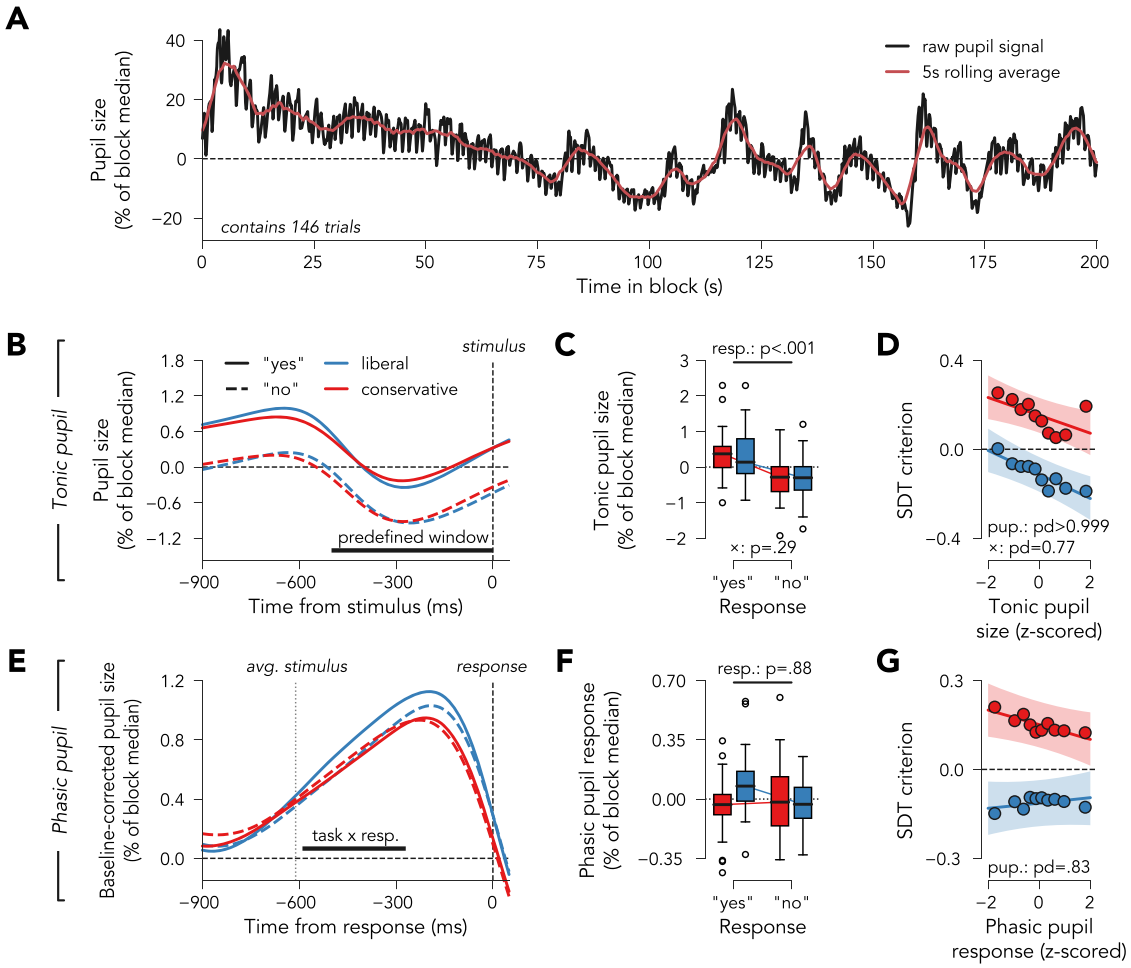

Fig. 2 | Phasic and tonic pupil-linked arousal are distinctly associated with decision bias. A Example pupil trace of 200 s of an example participant, containing 146 behavioral trials. Pupil size fluctuates substantially on a relatively slow timescale, e.g., in the first 100 s the pupil constricts from around 40% of the block median to −10% of the block median. On top of these slow drifts in pupil size, more frequent and relatively small pupillary responses can be observed, evoked by task-related events (stimuli, responses). **B** Average stimulus-locked pupil traces, split up for behavioral response ("yes"/"no") and task (liberal/conservative). The black horizontal bar indicates the predefined time-window that was used to extract tonic pupil-linked arousal. **C** Mean pupil sizes from the cluster shown in (**B**), for both tasks and behavioral responses (normalized by subtraction of grand average pupil size for visualization purposes). Tonic pupil-linked arousal was increased for "yes" vs. "no" responses (demarked with resp.), but there was no interaction effect between task and response (demarked with ×). **D** Empirical SDT criterion calculated for 10 tonic pupil bins (circles) and fit of Bayesian GLM-SDT model (fit to z-scored tonic pupil-linked arousal). Note that although the plot shows 10 tonic pupil bins, continuous data were used as input for the Bayesian GLM-SDT. pup.: main effect tonic pupil-linked arousal, ×: interaction between task and tonic pupil-linked. **E** Same as (**B**), but for the (baseline-corrected) response-locked phasic pupil response. Black horizontal bar indicates significant interaction effect between task and behavioral response. **F** Mean pupil sizes from the cluster shown in the (**E**), for both tasks and behavioral responses (normalized by grand average pupil response for visualization purposes). **G** Same as (**D**), but for phasic pupil responses. Note that no statistics are reported for task x response (**F**) and task x phasic pupil response (**G**) interaction effects, as the phasic pupil response was calculated from the cluster shown in (**E**), in which there was a significant task x response interaction.

−20% signal change with respect to the block median), happening in the order of minutes, across multiple trials. On top of these slow pupil dynamics there are transient changes in pupil size (in the order of ±5% signal change with respect to the block median), likely related to stimulus presentation, behavioral responses, and various cognitive processes.

Recently, tonic pupil-linked arousal was shown to correlate with perceptual sensitivity in multiple sensory modalities (visual, auditory) and decision types (discrimination, detection)[21], but how it relates to the criterion is less clear, although tonic pupil-linked arousal has been shown to be larger for "yes" vs. "no" answers[18,25]. To investigate whether fluctuations in tonic pupil-linked arousal were related to inherent and strategic decision bias, tonic pupil-linked arousal was calculated as the average pupil size in the 500 ms preceding stimulus onset for every trial (Fig. 2B; an identical time-window was used in earlier work from our group[21,23,51]). A 2×2 (task x response) repeated measures (rm)ANOVA revealed that "yes" responses were preceded by increased tonic pupil-linked arousal compared to "no" responses ($F(1,27) = 16.10$, $\eta_p^2 = 0.37$, $p < 0.001$, $BF_{01} = 0.02$; Fig. 2C). In contrast, there was no interaction effect between task and response in terms of tonic pupil-linked arousal ($F(1,27) = 1.17$, $\eta_p^2 = 0.04$, $p = 0.29$, $BF_{01} = 2.16$; Fig. 2C). Next, a similar hierarchical Bayesian GLM-SDT analysis as reported in Fig. 1D was constructed, with task and single-trial (z-scored) tonic pupil-linked arousal as predictors of SDT d' and criterion (see Methods). The model revealed that tonic pupil-linked arousal exhibited an overall negative relation with SDT criterion ($pd > 0.999$, $\mu = -0.05$, $\sigma = 0.01$, $CI_{95\%} = [-0.07, -0.02]$; Fig. 2D; posterior in Supplementary Fig. 3A), but that there was no interaction effect between tonic pupil-linked arousal and task ($pd = 0.77$, $\mu = 0.01$, $\sigma = 0.01$, $CI_{95\%} = [-0.01, 0.03]$; Fig. 2D; posterior in Supplementary Fig. 3B). In sum, tonic pupil-linked arousal was increased for "yes" versus "no" responses and exhibited a negative relation with criterion, but strategic shifts in criterion did not scale with tonic pupil-linked arousal.

Phasic pupil-linked arousal related to strategic shifts in bias, but not to inherent bias

Previously, transient (response-locked) phasic pupil responses have been related to a reduction in decision bias (i.e., less biased behavior) across decision domains and animal species[18,25,26]. In Fig. 2E, the response-locked pupil response is shown for each task and behavioral response (see Methods). These traces were derived by calculating the average pupil response for hits, misses, false alarms, and correct rejections and then averaging over these conditions, depending on the behavioral response (i.e., average of hits and false alarms vs. average of misses and correct rejections). Consequently, these response-contingent signals were not related to task performance or stimulus information, but solely reflected pupil dynamics underlying the "yes" vs. "no" decision. A permutation-based cluster-corrected 2×2 (task x response, cluster-threshold: $p < 0.05$, 10.000 permutations) rmANOVA over time revealed an interaction between task and response in phasic pupil-linked arousal from −590 ms to −270 ms before the response (p = 0.02; Fig. 2E). At these times, phasic pupil-linked arousal was increased for responses that violated the decision bias induced by the task (Fig. 2F). For example, during the conservative task—in which participants were biased towards providing "no" responses– phasic pupil-linked arousal was highest for "yes" responses. Within this time-window, there was no main effect of response on phasic pupil-linked arousal ($F(1,27) = 0.02$, $\eta_p^2 = 0.00$, $p = 0.88$, $BF_{01} = 3.93$; Fig. 2F). This effect was not driven by condition differences in RT (Supplementary Fig. 4).

Next, for each trial, phasic pupil-linked arousal was calculated as the average (normalized) pupil size between −590 ms and −270 ms. Then, another SDT-GLM model was fit to single-trial data, but now with task and single-trial (z-scored) phasic pupil-linked arousal as predictors. The model showed that phasic pupil-linked arousal did not correlate with overall SDT criterion (pd = 0.83, $\mu = -0.01$, $\sigma = 0.01$, $CI_{95\%} = [-0.02, 0.01]$; Fig. 2G; posterior in Supplementary Fig. 3C). Thus, replicating previous work[18,25,26,28–30], strategic decision bias was reflected in phasic pupil-linked arousal.

Reflection of strategic bias in phasic pupil-linked arousal does not covary with pharmacological manipulations and tonic pupil-pupil-linked arousal

A substantial body of work has shown that the magnitude of task-evoked pupil responses tends to negatively correlate with tonic pupil size, with large tonic pupil sizes preceding small task-evoked responses and vice versa[18,25,26,52,53]. To exclude the possibility that the reflection of strategic decision bias in phasic pupil-linked arousal was not actually an inversion of an effect of tonic pupil-linked arousal, several control analyses were performed. In a first set of control analyses, the overall amplitudes of phasic pupil-linked arousal and spontaneous fluctuations in tonic pupil-linked arousal were compared to quantify their differences and interdependencies. The amplitude of phasic pupil-linked arousal was markedly smaller than the amplitude of fluctuations in tonic pupil-linked arousal (Supplementary Fig. 5A), did not correlate with tonic pupil-linked arousal (Supplementary Fig. 5B), and was not affected by ATX or DNP (Supplementary Fig. 5C). Thus, in the current dataset, phasic pupil-linked arousal captured a unique part of pupil dynamics, not confounded by spontaneous and pharmacologically induced changes in tonic arousal.

The second set of control analyses further confirmed that strategic decision bias was selectively reflected in phasic pupil-linked arousal and not modulated by spontaneous changes in tonic pupil-linked arousal or pharmacologically induced increases in tonic neuromodulator levels. First, after regressing out trial-by-trial fluctuations in tonic pupil-linked arousal from phasic pupil-linked arousal, the interaction between task and response was still significant (Supplementary Fig. 5D). Second, the reflection of task-related decision bias in phasic pupil-linked arousal did not scale with tonic pupil-linked arousal (Supplementary Fig. 5E). Third, neither ATX nor DNP altered the reflection of strategic decision bias in phasic pupil-linked arousal as compared to PLC (Supplementary Fig. 5F).

In sum, strategic decision bias was uniquely reflected in phasic pupil-linked arousal, not tonic pupil-linked arousal, and this relation was neither affected by pharmacological elevations of catecholaminergic and cholinergic levels, nor by slow spontaneous fluctuations in tonic pupil-linked arousal. Because tonic pupil-linked arousal did not show systematic relations with our task manipulations, the subsequent analyses focus on the computational and neural correlates of the interaction between phasic pupil-linked arousal and strategic decision bias. For completeness, comparisons with tonic pupil-linked arousal are reported when they aid the interpretation of the results.

Phasic pupil-linked arousal associated with weakened computational starting-point bias

Perceptual decisions are often formalized as a gradual accumulation of noisy sensory evidence towards an internal decision threshold[54,55]. To assess whether the phasic pupil-linked arousal modulations of strategic decision bias were related to alterations in evidence accumulation, a stimulus-coded DDM was fitted to choice behavior data[56]. Although evidence accumulation processes are often studied using slow-paced experiments with long stimulus durations that encourage participants to accumulate evidence (e.g., random dot motion kinematogram task with >1 s of stimulation[57]), behavioral and neural markers of evidence accumulation have also been observed during tasks with stimulus durations ~200 ms (as in the current experiment) and even as short as 30ms[23,33,58–61].

To assess whether participants engaged in decision processes compatible with evidence accumulation—rather than using different decision strategies (e.g., extrema detection[62])—we first inspected the centroparietal positivity component (CPP) as a neural marker commonly associated with unsigned evidence accumulation[63,64] (but see Discussion). Three features of the CPP were consistent with an accumulation-like process during the detection task (Fig. 3A–D). First, the response-locked CPP displayed a gradual build-up in amplitude that peaked around the time of the response. Second, the slope of the response-locked CPP was significantly increased in the 200 ms preceding the behavioral response for fast versus slow RT trials (median split; $t(27) = 3.53$, $p = 0.002$, $d = 0.47$, $BF_{01} = 0.04$). Third, CPP slope was increased for target present versus target absent trials ($F(1,27) = 20.15$, $\eta_p^2 = 0.43$, $p < 0.001$, $BF_{01} = 0.83$) and for correct versus incorrect trials ($F(1,27) = 72.33$, $\eta_p^2 = 0.73$, $p < 0.001$, $BF_{01} = 5.82e^{-13}$), but was not different for "yes" versus "no" responses ($F(1,27) = 2.38$, $\eta_p^2 = 0.08$, $p = 0.13$, $BF_{01} = 1.18$). These neural patterns indicated that the task elicited decision-related build-up dynamics compatible with sequential-sampling models, thereby affording the following DDM analysis.

The DDM was stimulus-coded, meaning that the upper and lower decision thresholds respectively reflected the two response options, "yes" vs. "no". This subclass of DDMs explains biased decision-making through changes in the starting point of the accumulation process (closer or further away from a specific decision boundary), a linear offset in drift rate (increased or decreased towards a specific decision boundary) referred to as drift criterion, or a combination of these effects (Fig. 3E, see also refs. 18,45,56). Although both parameters can induce a shift in the overall proportion of "yes" vs. "no" responses, they can be discerned on the basis of RT distributions for both responses[56]. To increase robustness, the model was implemented in a hierarchical Bayesian manner via the HDDM Python package[65]. Drift rate (v), non-decision time ($t0$), decision boundary separation (a), starting point (z) and drift criterion (v_{bias}) were included as latent parameters in the model and were all allowed to fluctuate with behavioral task phasic pupil bin, and their interaction. Finally, inter-trial drift rate variability was included in the model to enhance the model fit. Simulated data from this model fitted the empirical data well (Supplementary Fig. 6).

As expected based on earlier work[45], drift criterion was lower under the conservative task compared to the liberal task (pd > 0.999, $\mu = -0.15$, $\sigma = 0.04$, $CI_{95\%} = [-0.23, -0.08]$; 3F—upper left panel). This shows that strategic decision bias related to an increased rate of evidence accumulation

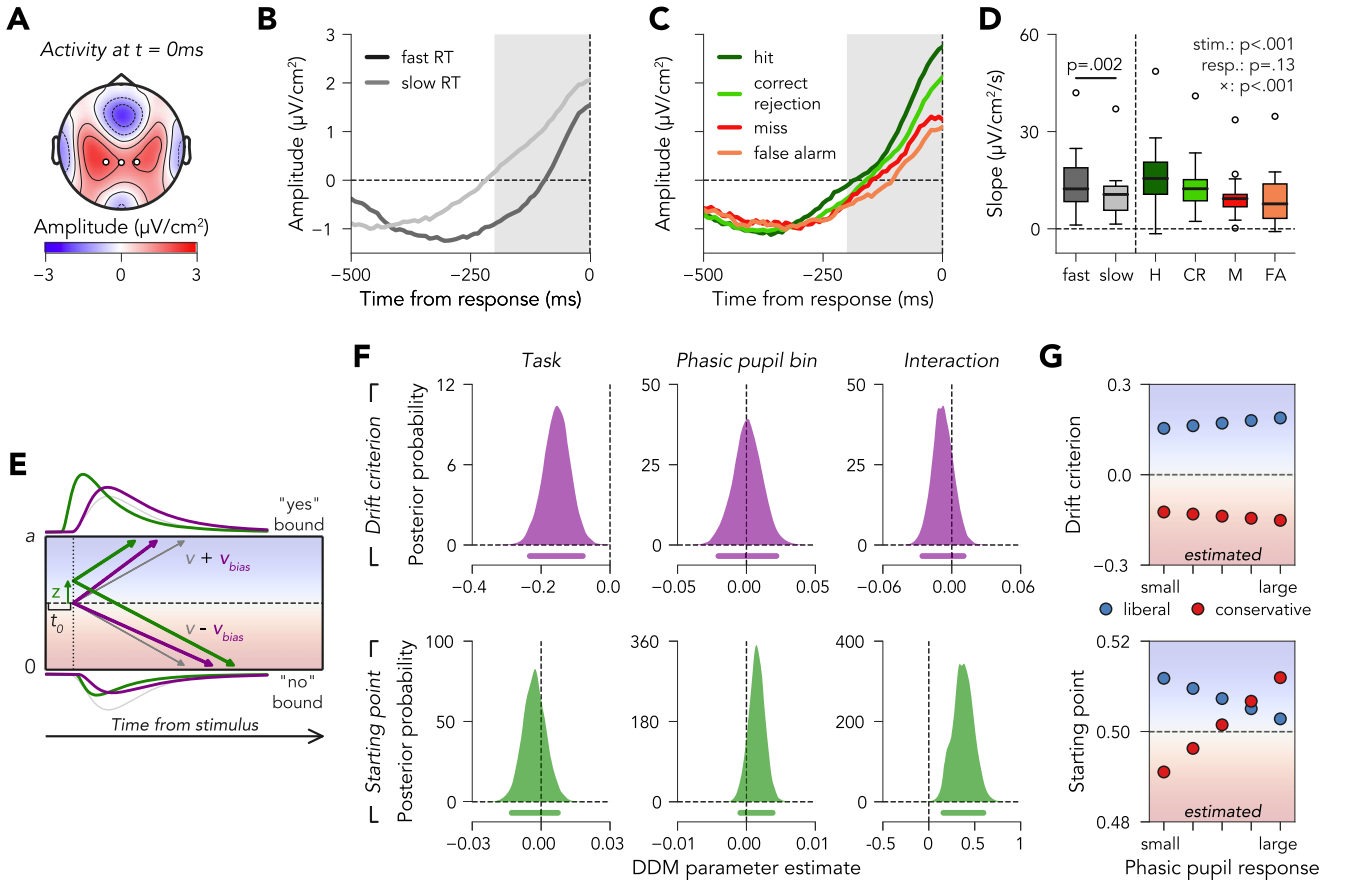

Fig. 3 | Strategic decision bias related to computational indices of biased evidence accumulation that are modulated by phasic pupil-linked arousal. **A**–**D** Centroparietal positivity component reveals evidence accumulation during decision-making. **A** Centroparietal ROI used to calculate the response-locked CPP. **B** Response-locked CPP for fast versus slow RT trials (median-split) and **C** for hits, correct rejections, misses, and false alarms. The gray area indicates the temporal window used to calculate the CPP slope. **D** Average CPP slopes in the 200 ms preceding the onset of the behavioral response for fast trials, slow trials, hits (H), correct rejections (CR), misses (M), and false alarms (FA). **E** Schematic representation of the origins of decision biases in the DDM. Decision bias can be brought about by changing the starting point of the accumulation process (z, in green) or adding an evidence-independent constant (drift criterion, v_{bias}, in purple) to the drift rate. **F** Posterior distributions of the effects of (from left to right) the behavioral task, phasic pupil bin, and their interaction on parameters underlying biased decisions. Top row: effects on drift criterion. Bottom row: effects on the starting point. Horizontal line on the bottom of the plot demarks the $CI_{95\%}$. **G** Top panel: reconstructed drift criterion values for each task (liberal task in blue, conservative task in red) and phasic pupil bin. Depicted values were calculated from the group-level posterior means of the model intercept and regressor weights. Bottom panel: similar to above, but for the starting point.

towards the decision bound of the preferred response. In contrast, phasic pupil bin was neither related to drift criterion overall (pd = 0.54, $\mu = 0.00$, $\sigma = 0.01$, $CI_{95\%} = [-0.02, 0.02]$; Fig. 3F—upper middle panel), nor to the effect of behavioral task on drift criterion (pd = 0.80, $\mu = -0.01$, $\sigma = 0.01$, $CI_{95\%} = [-0.03, 0.01]$; Fig. 3F—upper right panel). The starting point of evidence accumulation was not affected by task (pd = 0.72, $\mu = 0.00$, $\sigma = 0.01$, $CI_{95\%} = [-0.01, 0.01]$; Fig. 3F—lower left panel) and did not relate to phasic pupil bin (pd = 0.90 $\mu = 0.001$, $\sigma = 0.001$, $CI_{95\%} = [-0.001, 0.004]$; Fig. 3F—lower middle panel). Crucially, however, there was a significant interaction between task and phasic pupil bin in terms of accumulation starting point (pd > 0.999, $\mu = 0.004$, $\sigma = 0.001$, $CI_{95\%} = [0.002, 0.006]$; Fig. 3F—lower right panel). To further illustrate these effects, Fig. 3G shows reconstructed estimates for drift criterion (top row) and starting point (bottom row) for each task and across phasic pupil bins. As can be seen from the converging lines, starting-point bias is minimized on trials with strong phasic pupil-linked arousal. Posterior distributions for all model parameters (including *v*, *t0*, *a*) and experimental conditions (phasic pupil bin x task) are shown in Supplementary Fig. 7.

To summarize, the behavioral task (error type punishment) biased the rate of evidence accumulation towards the decision bound of the preferred response, but this effect was not modulated by phasic pupil-linked arousal. Moreover, neither the task nor phasic pupil-linked arousal exerted a main effect on the starting point of the accumulation process. Critically, the crossover interaction effect revealed that high phasic pupil-linked arousal transiently reduced starting-point bias, suggesting that it mitigates task-induced biases in the initial stages of decision formation.

Preparatory low-frequency activity over motor cortex underlying strategic bias shifts is negatively correlated with phasic pupil-linked arousal

Because the CPP is unsigned with respect to the behavioral response, it is not well-suited for investigating response-selective modulations by the behavioral task and phasic pupil responses. For that purpose, we turned to response-selective preparatory neural signals, which can be measured as lateralized activity over motor cortex in the delta-band (1 Hz to 4 Hz), theta-band (4 Hz to 8 Hz), and beta-band (~ 18 Hz to 30 Hz) ranges[66–72]. The difference between signal strength over the left motor cortex (related to "yes" responses made with the right hand) and right motor cortex (related to "no" responses made with the left hand) thus reflects a neural measure of response preparation (Fig. 4A). In the following section, lateralized activity over motor cortex is inspected to investigate if and how preparatory activity over motor cortex correlated with task, phasic pupil responses, and their interaction.

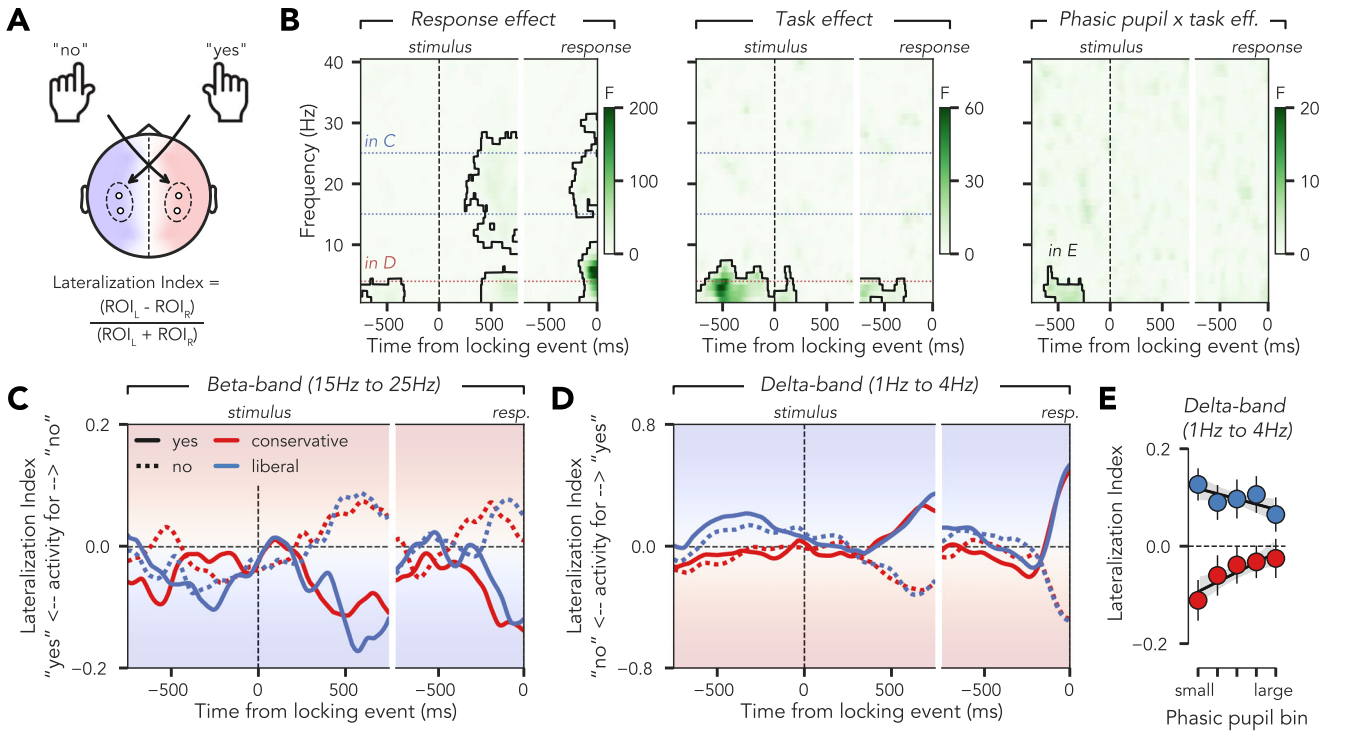

Fig. 4 | Lateralized low-frequency activity over motor cortex tracks strategic decision bias and scales with phasic pupil-linked arousal. A Two symmetrical spatial ROIs over the motor cortex were used to calculate lateralized TF power. As responses were always given with the same hand, activity over the left motor cortex was always associated with "yes" responses and activity over the right motor cortex was always associated with "no" responses. **B** Effects of (from left to right) the behavioral response, task, and the interaction effect between phasic pupil bin and task on lateralized activity over motor cortex. Figures show F-statistic obtained from a cluster-corrected 2 × 2 × 5 (task x response x phasic pupil bin) rmANOVA across the TF spectrum. Clusters that survived thresholding ($p < 0.05$) are demarked in black. **C** Stimulus-locked and response-locked lateralized activity in the beta-band (15–25 Hz) for each task and behavioral response. **D** The same as (**C**), but for lateralized delta-band (1 Hz to 4 Hz) activity. Before stimulus onset, the liberal task was clearly associated with stronger delta-band activity related to "yes" responses as compared to the conservative task. **E** Lateralized activity from the task x phasic pupil bin interaction cluster (**B**) for each task and phasic pupil bin. Error bars indicate SEM.

To obtain response-selective neural signals that were unaffected by spillover effects from the previous response on the current trial, trial counts of stimulus-locked and response-locked EEG epochs were first balanced with regard to the behavioral response on the previous trial, within each task. Note that regressing out the previous response from time-domain EEG data, instead of balancing trial counts, did not affect the results (Supplementary Fig. 8). Next, EEG data were averaged in a similar fashion as the pupil traces in Fig. 2 to extract neural signals specifically related to the behavioral response, not contaminated by stimulus information or choice accuracy. Additionally, epochs were grouped and averaged within each phasic pupil bin. This binning procedure was performed within each drug session, task, and block of the task to exclude the possibility that certain pupil bins contained more/less trials from a specific drug condition (e.g., ATX increased pupil size). An identical approach was used in earlier work from our group[21,23,51]. These averaged data were then decomposed into time-frequency (TF) power (see Methods). Lateralized activity was obtained by extracting TF power from two symmetrical, unilateral spatial regions of interest (ROIs; left hemisphere: C3 and CP3, right hemisphere: C4 and CP4; Fig. 4A) and then calculating a lateralization index (see Methods). This lateralization index could take values between −1 and 1, with positive values reflecting stronger power over the left motor cortex (coding for "yes" responses made with the right hand) and vice versa for negative values. Lateralized TF power was obtained for neural data locked to the onset of the stimulus as well as to the behavioral response.

The effects of the behavioral response, task, and phasic pupil bin were tested on lateralized neural TF power with cluster-corrected 2x2x5 rmANOVAs (10,000 permutations). In line with previous work[66,67] the upcoming behavioral response was indeed reflected in lateralized activity over motor cortex in the beta-band (beta-band cluster: $p < 0.001$, 15 Hz to 31 Hz, −281 ms to 0 ms, response-locked; Fig. 4B—left panel) and delta/theta-band (delta/theta-band cluster: $p < 0.001$, 1 Hz to 10 Hz, −188 ms to 0 ms, response-locked; Fig. 4B—left panel). The upcoming behavioral response was also reflected in lateralized low-frequency power before stimulus onset ($p = 0.02$, 1 Hz to 4 Hz, −750 ms to −336 ms; Fig. 4B—left panel). The behavioral task robustly modulated lateralized activity over motor cortex before stimulus onset ($p < 0.001$, 1 Hz to 7 Hz, −750 ms to 203 ms, stimulus-locked) and this effect lasted until 281 ms preceding the behavioral response ($p = 0.01$, 1 Hz to 4 Hz, −750 ms to −281 ms, response-locked; Fig. 4B—middle panel). Crucially, the prestimulus effect of the behavioral task on preparatory lateralized activity was modulated by phasic pupil bin (task x phasic pupil bin interaction; $p = 0.02$, 1 Hz to 6 Hz, −633 ms to −258 ms, stimulus-locked; Fig. 4B—right panel). No other clusters survived threshold-correction.

To elucidate the direction of these effects, lateralized power from the beta-band (15 Hz to 25 Hz) and delta-band (1 Hz to 4 Hz) is shown in Fig. 4C, D for each task and behavioral response. In line with earlier work[67], beta-band activity was decreased over contralateral motor cortex for each response (e.g., negative lateralization index for "yes" responses; Fig. 4C). In contrast, delta-band activity was increased over contralateral motor cortex for each response (Fig. 4D). The liberal task was furthermore associated with more positive lateralized delta-band activity before stimulus onset, corresponding to enhanced neural activity for "yes" decisions, and vice versa for the conservative task (Fig. 4D). This effect thus reveals prestimulus preparatory delta-band activity over motor cortex corresponding to the preferred behavioral response. Crucially, the interaction effect between behavioral task and phasic pupil bin on lateralized low-frequency power

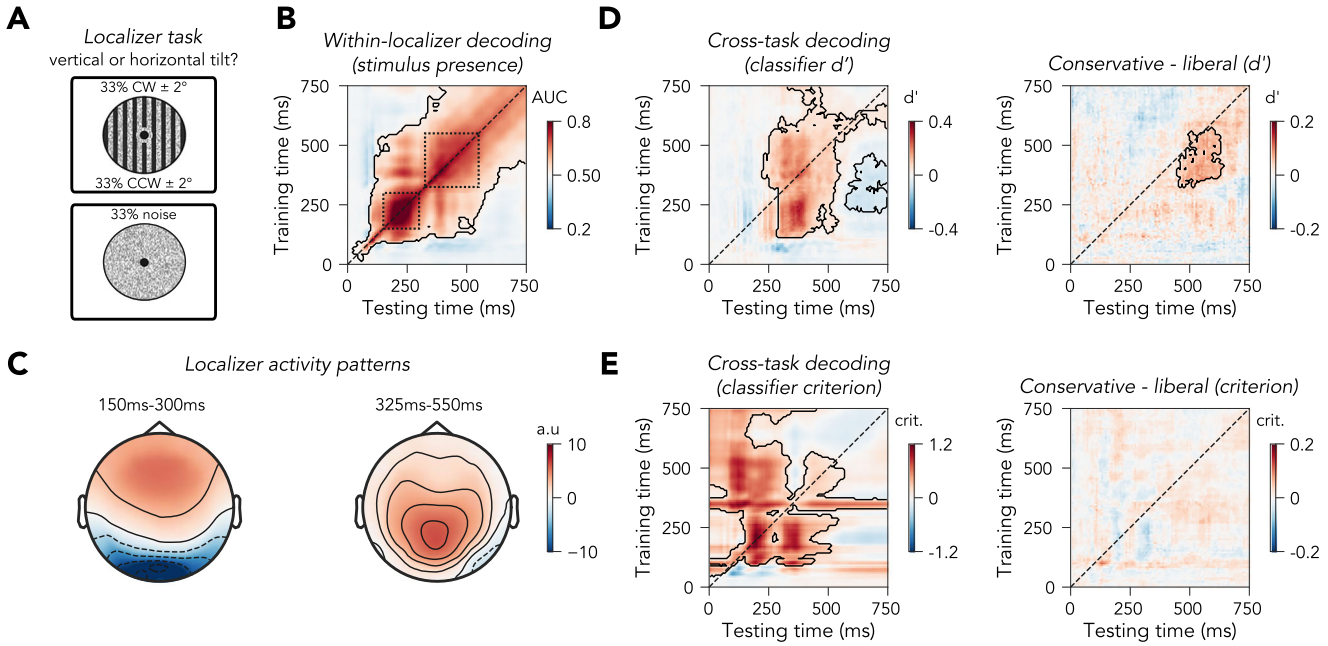

Fig. 5 | Strategic shifts in decision bias alter the precision, but not bias, of sensory representations in neural activity. A Schematic of the localizer task. Participants reported whether Gabor stimuli were presented closer to the horizontal or vertical axis; thus, responses and stimulus presence were orthogonal. **B** Within-localizer task 10-fold stimulus presence decoding (area under the curve, AUC). Squares demarked in dashed black lines indicate the temporal ROIs used for the reconstruction of spatial activity patterns. **C** Reconstructed activity patterns of the localizer task on early (150 ms–300 ms) and later timepoints (325–550 ms). **D** Left panel: classifier d' averaged across tasks. The classifier was able to decode stimulus presence above chance level (d' > 0). Right panel: Classifier d' was increased under the conservative versus liberal task. **E** Left panel: classifier criterion averaged tasks. Across tasks, the classifier had a conservative decision bias, i.e., it was biased towards classifying trials as containing a noise stimulus. Right panel: Classifier criterion was not modulated by task.

over motor cortex reveals that the effect of behavioral task on prestimulus lateralization became smaller with increased phasic pupil responses (Fig. 4E), mirroring the interaction between task and phasic pupil in terms of SDT criterion (Fig. 2G).

Both beta-band and delta-band lateralized activity did not, however, reflect evidence accumulation in the current dataset, because the slopes of both signals were not different for fast versus slow decisions (Supplementary Fig. 9). Lateralized delta-band, but not beta-band, activity did reveal delayed stimulus-locked peak latencies as well as decreased response-locked peak amplitudes for slow versus fast trials, suggesting that delta-band lateralization reflected motor preparation or decision urgency signaling[73–76].

Thus, adopting a more liberal or conservative decision criterion results in changes in preparatory prestimulus lateralized activity over motor cortex that is in line with the preferred behavioral response. This preparatory neural activity was weakest on trials with strong phasic pupil-linked arousal, in line with the negative correlation between phasic pupil-linked arousal and strategic decision bias.

Drug and tonic pupil-linked arousal do not modulate task effects on preparatory motor cortex activity

To explore the effects of drug condition and tonic pupil bin on preparatory signals over motor cortex, lateralized power over motor cortex was calculated in a similar fashion as above, but instead of extracting these signals within phasic pupil bin, they were obtained per drug condition or tonic pupil bin (5 bins, similar binning procedure as above). Next, cluster-corrected rmANOVA were performed separately for ATX versus PLC, DNP versus PLC, and for five tonic pupil bins. No clusters for a main effect of tonic pupil bin or an interaction between tonic pupil bin and task survived thresholding (all clusters $p > 0.34$). Following a similar approach to test whether drug condition affected lateralized activity over motor cortex also revealed no clusters in which there was a main effect of drug condition or an interaction effect between drug condition and task (ATX: all clusters $p > 0.51$; DNP: all clusters $p > 0.38$). Thus, contrary to phasic neuromodulatory responses, pharmacologically induced and spontaneous increases in tonic neuromodulator activity did not modulate the effect of strategic decision biases on preparatory activity over motor cortex.

Strategic shifts in decision bias show no reliable association with prestimulus frontal theta, occipital alpha, and biases in sensory processing

In a previous study in which aversive tones were presented to induce strategic decision biases in a visual detection task, the liberal task (vs. conservative task) was associated with increased prestimulus frontal theta-band power (2 Hz–6 Hz), reduced prestimulus occipital alpha-band power (8 Hz–12 Hz), and a weak increase in stimulus-locked occipital gamma-band power (59 Hz–100 Hz), suggesting that strategic biases may already arise at the earliest stages of sensory processing[45]. To test whether we could replicate these findings, we performed two sets of analyses: a spectral power analysis on prestimulus (−500 ms–0 ms) activity and a time-resolved multivariate decoding analysis on stimulus-locked activity. Prestimulus power was calculated within pre-defined frontal and occipital electrode clusters based on Kloosterman et al. (2019) and then tested using a hypothesis-driven (with respect to frequency) paired sample *t* test between tasks, as well as a hypothesis-free (with respect to frequency) cluster-corrected permutation test. We observed no task effects on frontal theta-band and occipital alpha-band activity (Supplementary Fig. 10).

Next, we trained a linear discriminant classifier (LDA) to distinguish Gabor stimuli from noise on EEG data obtained from an independent task performed by the participants (localizer task; see Methods, Fig. 5A). During the localizer, participants indicated offsets in the orientation, not the presence, of Gabor patches. Therefore, we could disentangle patterns of neural activity underlying the processing of the Gabor stimulus, independent of neural patterns related to response preparation and execution. The classifier was trained on each timepoint and tested across all other timepoints to investigate how patterns of activity underlying Gabor detection generalized over time[77]. A 10-fold within-localizer decoding procedure revealed that stimulus presence could be decoded from the localizer task with high accuracy ($p < 0.001$, training time: 16 ms–750 ms, testing time:

23 ms–750 ms, maximal cluster AUC = 0.87, mean cluster AUC = 0.62; Fig. 5B).

We then verified whether Gabor presence could be cross-decoded by training the classifier on data from the localizer task and testing it on data from the detection task. For every trial of the detection task, we obtained a classifier response ("yes" or "no"), which we could match to objective stimulus presence to obtain classifier hits, false alarms, misses, and correct rejections. This facilitated calculating classifier sensitivity (d') and bias (criterion). These measures were then compared between the liberal and conservative tasks to investigate if sensory processing was altered. Across tasks, the classifier was able to predict stimulus presence above chance, indicated by $d' > 0$ ($p < 0.001$, training time: 117 ms to 750 ms, testing time: 227 ms to 750 ms, maximal cluster $d' = 0.33$, mean cluster $d' = 0.12$; Fig. 5D). In line with the behavioral results (d' task effects, Fig. 1D), classifier d' was increased for the conservative vs. liberal task condition ($p = 0.002$, training time: 328 ms to 570 ms, testing time: 453 ms to 641 ms, maximal cluster $d' = 0.10$, mean cluster $d' = 0.06$; Fig. 5D). The classifier had a strong conservative bias for classifying neural signals as reflecting noise, indicated by criterion > 0 ($p < 0.001$, training time: 47 ms to 750 ms, testing time: 0–748 ms, maximal cluster criterion = 1.19, mean cluster criterion = 0.48; Fig. 5E). Crucially, however, we observed no condition difference when comparing classifier criterion between the conservative and liberal tasks (all clusters: $p > 0.59$; Fig. 5E). This suggests that task effects on decision bias were likely not related to alterations in sensory processing in the current dataset.

Taken together, these analyses provide no evidence that strategic shifts in decision bias were accompanied by changes in prestimulus frontal theta or occipital alpha power, nor by alterations in sensory processing as assessed with cross-decoding. These results contrast with earlier findings[45]. We speculate on possible explanations for these differences in the Discussion.

Discussion

This study set out to uncover the computational and neural mechanisms by which phasic and tonic arousal govern decision bias. To this end, we combined experimental manipulations of decision bias with correlational measures of pupil-linked arousal and pharmacological interventions to increase tonic levels of the two primary neuromodulator systems that control arousal (catecholamines, acetylcholine).

Replicating earlier work[45,78], non-monetary punishments, following either misses or false alarms, induced robust strategic shifts in decision bias (Fig. 1D). Tonic (baseline) pupil size measurements showed no relationship with task-induced changes in strategic decision bias. Furthermore, although increased catecholaminergic drive (ATX) elevated physiological measures of arousal and cholinergic drive (DNP) did not, neither manipulation influenced strategic decision bias (Fig. 1B–D). Tonic pupil-linked arousal was negatively correlated to inherent decision bias, showing that decision-making becomes more liberal in high tonic arousal states, independent of task context (Fig. 2B–D). The pharmacological interventions revealed a trend in the same direction (Fig. 1D).

In sharp contrast, and in line with earlier work[18,25,26,28–30], phasic pupil-linked arousal predicted a reduction of strategic decision bias: unpreferred responses, e.g., "yes" in the conservative condition, were associated with the largest phasic pupil dilations (Fig. 2E). Neural and computational analyses further revealed that task effects on preparatory activity over motor cortex, resembling a starting-point bias, were smallest on trials with high phasic pupil-linked arousal (Figs. 4E and 6C). Stimulus processing was not biased towards the preferred stimulus category following strategic shifts in decision bias (Fig. 5). Together, these findings demonstrate that phasic and tonic pupil-linked arousal differentially shape human decision-making: tonic pupil-linked arousal covaries with context-independent inherent decision bias, whereas phasic arousal relates to reduced task-induced strategic bias linked to preparatory decision processes.

A growing body of research suggests that tonic pupil-linked arousal follows a non-monotonic, inverted-U type relation with perceptual sensitivity[17,21,22,24,31,51,79–82], whereas phasic arousal exhibits a linear negative correlation with decision bias[18,25–30]. Most causal evidence supporting this distinction comes from animal studies focusing on the two most prominent neuromodulatory systems that contribute to arousal: the noradrenergic LC and cholinergic basal forebrain (BaF). For example, in rats, sensory-evoked responses in the thalamus are strongest at intermediate levels of tonic electrical stimulation of LC, and response magnitudes taper off at the upper and lower extremes of LC stimulation[79]. Conversely, in mice, phasic optogenetic stimulation of BaF neurons results in both increased hit and false alarm rates of visual stimulus detection, whereas optogenetic inhibition of these neurons has the opposite effect, implicating phasic BaF activity in regulating decision bias[83].

However, the precise neural mechanisms underlying the distinct functional roles of tonic and task-evoked arousal on behavior are still being explored. We recently hypothesized that the inverted-U relation between tonic (pupil-linked) arousal and perceptual sensitivity may be (in part) related to modulations of interneuron chains in cortical microcircuits[21,51], possibly shaping the excitability of sensory systems[84], which may also be reflected in prestimulus oscillatory power in the alpha-band (~ 8hz to 12 Hz)[85]. Consequently, tonic arousal may enhance internal responses to both noise and target stimuli, inducing a more liberal decision criterion. In contrast, phasic arousal has been linked to rapid behavioral adjustments in the face of uncertainty or violated predictions, through a reset of cortical network dynamics and the promotion of bottom-up sensory processing over top-down influences[34–37,86–89]. The negative correlation between trial-by-trial variations in phasic pupil-linked arousal and strategic decision bias reported here is broadly consistent with these theoretical accounts. However, because our design did not explicitly manipulate predictions or uncertainty, it remains difficult to directly attribute the observed variability in phasic pupil-linked arousal to prediction-related processes. Although the observed effects of phasic arousal may have been partially driven by local stimulus patterns that occur by chance in pseudorandomized tasks (driving the formation of short-term predictions[90]), future work should test this hypothesis with designs optimized to probe such predictive mechanisms.

The computational and neural underpinnings of the relation between phasic arousal and decision bias may vary under different experimental conditions. For example, in an auditory yes/no detection task where target stimulus probability was systematically varied between 30%, 50%, and 70% across blocks to manipulate decision bias, phasic pupil-linked arousal correlated with drift criterion in all cases and with starting point only in the rare (30%) and frequent (70%) blocks[26]. Moreover, phasic pupil-linked arousal only correlated with drift criterion, and not with starting point, in a yes/no recognition task[26]. These divergent findings may indicate that phasic arousal differentially modulates various computational components underlying decision formation depending on task-context (drift criterion versus starting point), but they could alternatively reflect characteristics of the applied computational models. Specifically, DDMs distinguish effects on drift criterion and starting point based on the shape of RT distributions: starting point effects are reflected in both fast and slow RTs, whereas drift criterion effects manifest primarily in slow RTs[56]. This means that drift criterion effects depend on systematic variance in the tail of the RT distribution that can be explained by a covariate, e.g., phasic pupil-linked arousal. As RT duration was less restricted in De Gee et al. (2020) (in yes/no detection participants had 2500 ms to respond, and in yes/no recognition even 7500 ms from stimulus onset) compared to the current experiment (1400 ms from stimulus onset), RT distributions had wider tails, potentially facilitating the detection of drift criterion effects over starting point effects.

A complementary approach is to analyze neural data or using neurally informed computational models of choice behavior[73]. Here, EEG recordings with high temporal resolution revealed a relation between phasic pupil-linked arousal and prestimulus preparatory activity over motor cortex, consistent with a pre-accumulation starting point modulation (Fig. 4). However, the interpretation of EEG components as signatures of decision-related processes remains debated. Recent work using a deconvolution analysis suggests that the CPP may not solely reflect evidence accumulation, but instead comprises multiple overlapping sources, including stimulus-evoked activity[91]. In turn, others have argued that this deconvolution

approach is problematic and may obscure genuine accumulation-related activity[92]. Although the observed CPP signatures are consistent with evidence accumulation, they are not uniquely diagnostic and may reflect component overlap. Overall, our results thus provide a deeper understanding of the relation between decision bias and phasic pupil-linked arousal, but future work is needed to delineate the conditions under which phasic arousal affects evidence accumulation, pre-accumulation motor preparation, or both.

Phasic pupil-linked arousal negatively correlated with the task effect on preparatory lateralized low-frequency (< 7 Hz) activity over motor cortex (Fig. 4E). Previous research has shown that motor cortex intrinsically oscillates in both the delta-band (1 Hz to 4 Hz) and beta-band (~ 12 Hz to 30 Hz)[93] and that lateralized activity in these frequency bands predicts the upcoming motor response[67,72,94]. The specific mechanisms captured by these oscillatory measures are still being explored, but it has been hypothesized that delta-band oscillations are entrained to predictable task-relevant events and consequently modulate the amplitude of beta-band oscillations around these task-relevant events[95]. Moreover, expectations about the upcoming stimulus (and associated motor response) are reflected in prestimulus lateralized activity between 8 Hz to 30Hz[66] (note that frequencies <5 Hz were not analyzed in this study). These findings suggest that oscillatory activity in motor cortex is related to the anticipation of specific movements and their precise timing. The robust modulation of prestimulus activity over motor cortex by the task observed in the current study is in line with this idea, as the motor system may anticipate making more "yes" versus "no" decisions when missed targets are punished.

Previous work, using a similar manipulation of strategic decision bias during a visual detection task, revealed that strategic shifts in decision bias were accompanied by prestimulus changes in frontal theta and occipital alpha power, as well as alterations in stimulus-evoked occipital gamma power suggestive of biased sensory processing[45]. We did not observe these neural patterns in our data (Fig. 5). This discrepancy may be related to several methodological differences between our study and Kloosterman et al. (2019). First, in Kloosterman et al. (2019), participants only reported the presence and not the absence of visual target stimuli. Consequently, participants in that study may have used a different strategy to implement criterion shifts as compared to ours. Indeed, participants also exhibited more conservative choice behavior averaged across tasks in their study (average *c* was ~0.30 in Kloosterman et al. (2019) versus ~0.03 in our study). Second, the used stimuli were different. We presented Gabor patches embedded in dynamic visual noise on 50% of all trials, and neither trial start nor stimulus onset was cued. In contrast, Kloosterman et al. (2019) presented orthogonal orientation-defined squares ('figure-ground stimuli') on 75% of all trials in a continuous rapid serial visual presentation, with preceding and subsequent masking stimuli being presented at 25 Hz. Target stimulus onset was also not cued, but it could occur at different moments in the visual stream, hampering the anticipation of exact stimulus presentation and response preparation. This difference in temporal structure may have shifted neural mechanisms from frontal control over sensory excitability, as observed in Kloosterman et al., towards prestimulus response preparation in our study. Furthermore, they used monetary penalties in addition to the aversive tones, and this motivational context may have amplified strategic shifts in decision bias in their study (task effect on *c* was ~0.80 in Kloosterman et al. versus ~0.28 in our study). Finally, the window over which we could compute the prestimulus power in our study was smaller than that in Kloosterman et al. due to task design differences (500 ms vs 1000 ms). Taken together, the divergent neural signatures accompanying strategic shifts in decision bias in the two studies may be due to differences in behavioral task demands, task structure, stimulus characteristics, motivational context, or effect size.

The directionality of the relation between phasic-pupil-linked arousal and strategic decision bias, motor cortex lateralization, and starting-point bias is hard to establish (e.g., pupillary effects preceded neural effects). First, all pupillary analyses were correlational, preventing conclusions about causality. Second, the pupillary response is relatively slow, almost akin to fMRI-BOLD responses[52,96], which makes it challenging to precisely align the timing of pupil-linked arousal with rapid changes in decision-related neural activity. Our current data, therefore, do not allow us to distinguish between a scenario in which pupil-linked phasic arousal minimizes strategic shifts in starting-point bias and one in which overcoming task-induced starting-point bias triggers phasic arousal. To causally establish whether trial-to-trial variations in phasic pupil-linked arousal or neuromodulator activity affect computational and neural markers of (strategic) decision bias, causal interventions with a relatively high temporal resolution are necessary. Recent examples of such manipulations include (transcutaneous) vagus nerve stimulation[53,97–99] and the presentation of arousing task-irrelevant stimuli[28,100]. Future applications of such methods may be required for firmly establishing the role of phasic arousal in decision bias.

Administration of 5 mg DNP did not produce any statistically robust physiological, behavioral, and neural effects. This is in line with our observations from two previous studies performed in the same group of participants[23,33]. It is difficult to retrospectively ascertain whether this absence of effects was due to a non-existent role for the cholinergic system in visual detection or was due to pharmacological properties such as the used dosage. However, there is a growing body of work suggesting that 5 mg DNP may mostly shape cortical activity at rest[101–103]. For example, this dosage of DNP minimizes the spread of visually evoked activity over visual regions when passively viewing flickering stimuli[103] and reduces cortex-wide inter-regional functional connectivity during resting-state measurements but not during an active task[101]. Pfeffer et al. (2018) further speculated that the absence of DNP effects during behavioral tasks may be related to the fact that the cholinergic system mostly operates through phasic transients (by e.g., modulating neural gain), rather than through long-lasting tonic effects. This would be in line with a recent reconceptualization of the forebrain cholinergic system, which claimed that likely all behaviorally relevant cholinergic signaling is phasic in nature[104]. One way to establish the role of either tonic or phasic cholinergic activity in the regulation of decision biases might be to antagonize the cholinergic system (with e.g., scopolamine or bupropion). For example, cholinergic antagonization might cause a weakened relation between phasic pupil-linked arousal and strategic decision biases, which would imply a role for phasic cholinergic signaling in shaping strategic decision bias.

In contrast to the absence of effects of ATX on d' in the current study (Fig. 1D), ATX was previously shown to significantly increase d' during two visual discrimination tasks in the same group of participants[23,33]. This intriguing differentiation seems in line with two previous studies. First, reboxetine, a catecholaminergic agonist, increased d' during a discrimination task in the absence of effects during a detection task[32] (note that antagonizing noradrenaline did decrease d'). Second, during drowsiness (a low-arousal state), the slope of psychometric curves decreased more strongly for discrimination than for detection tasks[105]. Thus, both studies suggest that the effect of neuromodulation on d' differs between discrimination and detection tasks. It is, to our knowledge, unknown what drives this difference. Speculatively, the effects of ATX on d' may depend on signal strength, which is known to be increased for detection tasks compared to discrimination tasks when behavioral performance is matched[106,107]. Indeed, the titrated Gabor contrast values of the current study were significantly higher than the discrimination contrasts used in Nuiten et al. (2024) (detection=0.037, discrimination=0.029; $t(27) = 8.13$, $p < .001$, $d = 1.21$, $BF_{01} = 7.55e^{-7}$), in the absence of a significant difference in decision accuracy (detection=77.37% ±6.56%, discrimination=76.05% ±7.33%; $t(27) = 0.81$, $p = 0.43$, $d = 0.19$, $BF_{01} = 3.70$). Note, however, that recent work from our lab has demonstrated that the relation between tonic pupil-linked arousal and d' is non-monotonic for both discrimination tasks and detection tasks[21,51]. Thus, arousal seems to modulate d' in both detection and discrimination, but perhaps the magnitude of this modulation may differ due to differences in, for instance, signal strength.

Methods

Participants

This study was part of a larger project including several study parts, some of which have been reported previously[23,33]. The current set of analyses has not

been published yet, although this data set has been part of a previous publication focusing on a different research question[21]. For this project, 30 healthy male participants (aged 18–30) were recruited from the online research environment of the University of Amsterdam. Participants underwent extensive screening, consisting of physiological measures (BMI, heart rate, and blood pressure), an electrocardiogram (ECG), and a psychiatric questionnaire to assess mental health. Participants were only included in the study following approval of the screening data by our study-associated physician. Written informed consent was obtained from all participants during the intake session following explanation of the experimental protocol, but preceding the screening procedure. Participants were not taking any psychotropic medication (other than the study medication) at the time of the study. Two participants decided to withdraw from the experiment after having performed the first experimental session. The data from these participants were not included in this work, resulting in $N = 28$. This study was approved by the Medical Ethical Committee of the Amsterdam University Medical Center and the local ethics committee of the University of Amsterdam. All ethical regulations relevant to human research participants were followed. Participants received monetary compensation for participation in this study.

Pharmacology and administration protocol

The study used a within-subject, randomized, double-blind crossover design. Atomoxetine (40 mg; ATX), donepezil (5 mg; DNP) and placebo were administered orally in separate experimental sessions, separated by a minimum of 7 days to allow for washout. The order of drug administration was counterbalanced between participants. Experimental days started at 09:00 and ended at 16:00. ATX is a relatively selective noradrenaline reuptake inhibitor, which increases noradrenaline and dopamine levels in the synaptic cleft[108]. The half-life of ATX varies between 4.5–19 hours and peak plasma levels are reached ~2 hours after administration. Donepezil is a cholinesterase inhibitor, which increases acetylcholine levels in the synaptic cleft. The elimination half-life of donepezil is 70 hours and peak plasma levels (T_{max}) are reached after ~4 hours[109]. Given the different durations after which DNP (~ 4 h) and ATX (~ 2 hours) reach peak plasma level in the blood, these pharmaceuticals were administered at different times prior to the onset of the behavioral tasks (DNP 4 hours before onset experiment, ATX 2 hours before onset experiment; Fig. 1A). To ensure the blinding of pharmacological condition, participants were administered two identical looking-pills each experimental session. The first pill (containing either PLC or DNP) was administered 4 hours before the onset of the behavioral task, and the second pill (containing either PLC or ATX) was administered 2 hours before the onset of the behavioral task. Thus, the drug administration schemes were as follows: ATX session (pill 1 = PLC, pill 2 = ATX), DNP session (pill 1 = DNP, pill 2 = PLC), PLC session (pill 1 = PLC, pill 2 = PLC). This administration scheme ensured that both ATX and DNP had reached peak plasma levels at the onset of the behavioral experiments, while participants remained blind to the specific drug condition of that session.

Physiological measurements were taken at three moments during each session: immediately before intake of the first drug, before onset of the first behavioral experiment (+ 4 hours), and at the end of each experimental session (+ 7 hours). Physiological measurements included heart rate and blood pressure. Additionally, participants indicated their subjective arousal levels by filling in a visual analog scale[110]. Tonic pupil size was assessed only once during each session, directly before the onset of the first experiment. Participants were presented with consecutive bright and dark screens (15 s each), and their minimal and maximal pupil size were quantified as the average pupil size during the final 5 s of the bright and dark monitor, respectively.

Experimental setting

An EEG apparatus was connected 30 minutes prior to the onset of the behavioral tasks. In total, participants performed five different computerized tasks while EEG measurements were made. The order of these behavioral tasks was counterbalanced between participants and maintained over sessions. Participants were seated in a darkened, sound-isolated room, 80 cm from a 69x39cm screen (frequency: 60 Hz, resolution: 1920 × 1080). The main task and staircase procedure were programmed in Python 2.7 using PsychoPy[111] and in-house scripts.

Gabor detection paradigm

Participants performed a visual detection task for which they had to report the presence of Gabor stimuli (radius 8.5°, spatial frequency 1.365 cycles/degree) that were presented on top of circular patches containing dynamic noise (radius 9.5°) for 200 ms (Fig. 1B). Gabor stimuli were presented on 50% of all trials and noise patches were always presented. So, in 50% of all trials, only noise was presented for 200 ms and in the other 50%, both noise and a Gabor were presented for 200 ms. Trial onset was not cued. Gabor stimuli could be oriented clockwise (CW, 45°) or counterclockwise (CCW, −45°) and orientation counts were equally distributed at 50%. Visual stimuli were presented on a static gray background. The centrally presented black circular fixation mark was visible throughout the experiment. Target absent answers were given by pressing the 'S' key on a keyboard with the left hand, target present answers were given by pressing the 'K' key with the right hand. Task difficulty (i.e., Gabor stimulus opacity) was determined for every participant during the intake session and was then fixed over all experimental sessions (see "staircasing procedure"). The response window started concurrently with stimulus presentation and lasted 1400 ms. If participants did not respond during this window, they would receive visual feedback informing them of their slow response (in Dutch: "te laat", which translates into: "too late"). A variable inter-trial interval (ITI) of (250 ms–350 ms, drawn from a uniform distribution) started directly after a response or at the end of the response-window.

Participants performed 960 trials of this task, divided into four blocks of 240 trials that were subdivided into mini-blocks of 80 trials. The bias manipulation was implemented by providing auditory feedback to specific types of errors. Specifically, an aversive buzzer tone (duration of 400 ms) was played directly following either false alarm trials (reporting stimulus presence, whilst it was absent) or missed trials (reporting stimulus absence, whilst it was present). Following each buzzer tone, an additional 500 ms was added to the ITI. These auditory feedback stimuli are referred to as punishments, although they were not related to any sort of punishment (e.g., monetary). Participants were not informed of the details of this manipulation or the specific condition they were in at any moment, but were instructed to minimize the number of buzzer tones. The aim of punishing false alarms was to make participants more cautious in their response strategy, inducing a conservative bias. Conversely, punishing missed target stimuli was expected to induce a more liberal bias. Bias was manipulated in a block-wise fashion, i.e., the first two blocks contained the same bias manipulation, and the final two contained the other manipulation. Task order was counterbalanced between participants but fixed across sessions.

Gaze position was monitored online to ensure participants' gaze remained at or near fixation (within 1.5°, horizontal axis, see "Data acquisition and preprocessing"). Trials on which fixation was lost, due to shifts in gaze or blinks, in the time interval from stimulus onset to the end of the response window, were marked as faulty. All faulty trials were appended as new trials at the end of each block, ensuring that eventually 240 usable trials were performed in each of the four blocks. A nine-point calibration was used at the start of each block. To minimise movement of the participant, a head-mount with a chinrest was used. Throughout the experiment, participants were instructed to move their heads as little as possible and to try to blink after they made their response.

Staircasing procedure

Participants performed a staircasing procedure during their intake session. After completing the staircasing procedure, task difficulty was fixed to be able to compare the effects of the pharmacological manipulation across all experimental sessions. The staircase task was almost identical to the primary task: stimulus properties, presentation time and response window duration were the same. The ITI was prolonged to 450 ms–650 ms. Participants

received feedback on their performance on a trial-by-trial basis; the fixation dot turned green for correct answers and red for incorrect answers. An adaptation of the weighted up-down method was used to staircase performance at 75% correct, by changing the opacity of the Gabor patch[112]. In short, corrections after erroneous responses were weighted differently than after correct responses, in a ratio of 3:1. The step-size was 0.01 (opacity scale: 0–1, 1 is fully opaque), thus after errors the opacity would be increased by 0.01 and after correct answers it would be decreased by 0.01/3. The procedure was aborted after 50 behavioral reversals, i.e., changes in sequences from correct to error or vice versa. The output difficulty of the staircase procedure was calculated as the average opacity on reversal trials. In total, participants performed two blocks of this staircase procedure. The first block started at a high opacity (0.15), allowing the participants to familiarize with the target stimulus. The second block started at the opacity obtained from the first block.

Localizer task

The localizer was similar to the visual detection task in terms of stimulus presentation times, response window duration, ITI, and stimulus characteristics (e.g. Gabor frequency and phase). During the localizer task, we centrally presented the same dynamic noise patches as during the main task. In 2/3 of all trials, we additionally presented Gabor patches on full opacity that could be oriented CW/CCW. The Gabor patches were slightly tilted by 2°, rendering them more vertical (± 43°) or more horizontal (± 47°) from diagonal (± 45°). Participants were required to report the tilt of the Gabor patches. Horizontally tilted stimuli were reported by pressing "S" on the keyboard with the left-hand index finger, vertically tilted stimuli were reported by pressing "K" with the right-hand index finger. If only a dynamic noise patch was presented, participants were asked to refrain from responding. In total, participants performed 840 trials, divided over two blocks of 420. The eyetracker was calibrated prior to block onset. Each block was subdivided into five mini-blocks of 84 trials each, allowing participants to rest or close their eyes (while keeping their head in the head-mount). Again, we excluded trials in which fixation was lost (> 1.5° from fixation or blink) and replaced these excluded trials to get to a total of 840 trials per session.

Data acquisition and preprocessing

EEG-data were recorded with a 64-channel BioSemi apparatus (BioSemi B.V., Amsterdam, The Netherlands), at 512 Hz. Vertical eye-movements were recorded with electrodes located above and below the left eye, horizontal eye-movements were recorded with electrodes located at the outer canthi of the left and the right eye. Gaze position and pupil size were measured with an EyeLink 1000 (SR Research, Canada) eyetracker during the experiment at 1000 Hz. All analyses were performed in Python 3.7.

Pupil preprocessing

All pupil traces were low-pass filtered with a cutoff frequency of 10 Hz, blinks were linearly interpolated, and effects of blinks and saccades on pupil diameter were removed via deconvolution[52]. Then, pupil traces were normalized as the percentage difference of the block median within each block of the experiment. Epochs were extracted by taking data from −2000 ms to 4000 ms locked to both the onset of the stimulus (stimulus-locked epochs) and response (response-locked) epochs. Finally, pupil epochs were resampled via decimation to 100 Hz.

EEG preprocessing

The MNE Python package (version 0.24.0) was used for most of our EEG analyses[113]. All EEG traces were re-referenced to the average of two electrodes located on the left and right earlobes. The data were high-pass filtered offline, with a cutoff frequency of 0.01 Hz. Next, bad channels were detected automatically via a random sample consensus algorithm (RANSAC), implemented in the Autoreject Python package[114]. This algorithm detects noisy channels based on correlations between simulated data (derived from data of a subset of epochs, averaged across channels) and the actual data of EEG channels. Channels with a low correlation score were marked as noisy, removed, and subsequently interpolated via spline interpolation. Next, epochs were created by taking data from −2000 ms to 2000 ms around the onset of stimulus presentation. To remove eyeblink artifacts, an independent component analysis (ICA; 25 components) was performed on the epoched data and components that strongly correlated to vertical EOG data were removed. In the liberal task, on average 1.33 (s.d. ±0.52, maximum: 2) components were rejected per file and in the conservative condition, on average 1.27 (s.d. ±0.47, maximum: 3) components were rejected per file. Remaining artifacts were automatically detected by using the same RANSAC algorithm as before, but on epoched data. Bad segments were repaired via interpolation if the artifactual data were present in only a few channels, but if more channels were affected, the epoch was removed from the EEG data. The automatic artifact rejection algorithm rejected on average 5.82% (s.d. ±7.90, maximum: 50.10%) of all epochs in the liberal task and 5.70% (s.d. ±5.89%, maximum: 26.53%) of all epochs were removed in the conservative task. Current scalp density (CSD) was computed as the surface Laplacian to attenuate the effects of volume conductance. Finally, epoched EEG data were downsampled to 128 Hz.

Data analysis

All behavioral analyses were programmed in Python 3.7. Trials which were marked due to lost fixation were disregarded from all analyses. Trials without a response and trials with a reaction time (RT) larger than 1400 ms and shorter than 200 ms were excluded from behavioral, pupillary, and EEG analyses. Note that data from all trials were used for analysis of behavioral and pupillary, but only unrejected (after automatic artefact rejection) EEG epochs were included in EEG analyses.

Analyses of physiological arousal and task effects

The maximal pupil size measurement was used to quantify drug effects on pupil size. For each active drug condition (ATX/DNP) tonic pupil size was normalized (percentage) to the tonic pupil size during the PLC session. Blood pressure was normalized (percentage) for each drug condition, including PLC, to the first measurement of each day. Next, two-sided t-tests were used to test for drug effects on blood pressure and tonic pupil. Bayesian equivalents of most statistical tests (Cauchy-scale=0.707) were used to quantify the evidence in favor of the null hypothesis. Bayesian tests were performed in JASP[115]. Note that all Bayes Factors (BF) are reported as evidence in favor of the null hypothesis (BF_{01}) and can be interpreted as anecdotal ($1 < BF_{01} < 3$), substantial ($3 < BF_{01} < 10$), strong ($10 < BF_{01} < 30$) and very strong ($BF_{01} > 30$)[116]. Inversely, a $BF_{01} < 1$ should be interpreted as evidence for the alternative hypothesis following the formula:

$$BF_{01} = \frac{1}{BF_{10}} \quad (1)$$

Thus, $0.10 < BF_{01} < 0.33$ should be considered substantial evidence in favor of the alternative hypothesis, $0.03 < BF_{01} < 0.10$ as strong evidence for the alternative hypothesis, etc.

Hierarchical generalized linear model formulation of signal detection theory

Perceptual sensitivity (d') and decision bias (criterion), derived from SDT[41], were estimated to investigate the effects of task and drug on behavior. Specifically, SDT was formulated as a probit regression model, which describes binary responses as a function of stimulus input and an intercept. In its most basics forms, this model is identical to standard SDT analyses[40]. The base SDT-GLM model is defined as follows.

$$\text{response} \sim \phi(\beta_0 + \beta_1 \cdot \text{stimulus}) \quad (2)$$

Where the intercept β_0 is equal to -criterion, β_1 is equal to d', and Φ indicates the cumulative standard normal that underlies the probit transform. For simplicity's sake, β_0 is multiplied by −1 so that it reflects the criterion in the

proper direction.

$$\begin{aligned}\text{response} \sim \phi(&\beta_0 + \beta_1 \cdot \text{stimulus} + \beta_2 \cdot \text{task} + \beta_3 \cdot \text{drug} \\ &+ \beta_4 \cdot \text{stimulus} \cdot \text{task} + \beta_5 \cdot \text{stimulus} \cdot \text{drug} \\ &+ \beta_6 \cdot \text{task} \cdot \text{drug} + \beta_7 \cdot \text{stimulus} \cdot \text{task} \cdot \text{drug})\end{aligned} \quad (3)$$

In this model, β_2 is the main effect of task on criterion, whereas β_4 is the main effect of task on d', etc. As described above, β_2, β_3, and β_6 were multiplied by −1 to obtain effects of task, drug and their interaction on the criterion in the correct direction. Model regressors were effect coded as −1 for the liberal task and the placebo, and 1 for the conservative task, the active drug condition (ATX or DNP). The model was implemented in a hierarchical Bayesian manner via the Python toolbox PyMC[117]. Model (hyper-) priors for the regressors were defined as follows:

$$\beta_{i,s} \sim \mathcal{N}(\mu_i, \sigma_i^2) \quad (4)$$

$$\mu_i \sim \mathcal{N}(0,\ 0.5) \quad (5)$$

$$\sigma_i^2 \sim \mathcal{HC}(0.5) \quad (6)$$

Where $\beta_{i,s}$ is the subject-level regressor i, μ_i and σ_i^2 indicate the hyperprior mean and variance for regressor i, $\mathcal{N}$ describes a normal distribution, and $\mathcal{HC}$ describes a half-Cauchy distribution. For $i = 1$ (i.e., β_1; grand mean of d'), the location of the hyperprior mean was set to 1.5 instead of zero, as performance on the task was titrated to ~75% correct, corresponding to a d' of ~1.5. Samples from the posterior distribution were found by running four Markov Chain Monte Carlo chains, each with a length of 10,000 and an additional 2000 burn-in samples. Regressors were effect-coded, meaning that effects should be interpreted as a difference from the grand mean (i.e., average across all conditions). The same modeling approach was used to estimate the effects of tonic pupil size and phasic pupil responses on behavior, also in interaction with task (see further explanation below). $\hat{R}$ was used as a metric for model convergence[118]. The ATX model, DNP model, tonic pupil model, and phasic pupil model converged well, with $\hat{R} \leq 1.005$ for all hyperparameters.

Pupillometry analyses and binning procedure

Tonic pupil size was calculated as the average pupil size in the 500 ms preceding stimulus onset (identical to refs. 21,23,51). Phasic pupil responses were calculated by 1) time-locking pupil traces to the onset of the behavioral response and 2) normalizing these traces by subtracting the tonic pupil size of that trial. To quantify how the task and the behavioral response were reflected in phasic pupil traces, single-trial response-locked pupil data were averaged within each participant, session, task, stimulus, and response. Next, pupil traces were averaged across sessions and stimuli to obtain pupil traces in a 2 × 2 (task x response) factorial design for each participant. Note that this procedure isolated pupil dynamics exclusively related to the decision ("yes" vs. "no"), uncontaminated by e.g., stimulus identity and decision accuracy.

Pupillary traces were analyzed with a 2 × 2 (task × response) cluster-corrected permutation rmANOVA over time (10,000 permutations, cluster-threshold: $p < 0.05$), in which the interaction between task and response was of primary interest, as that interaction should reflect strategic decision bias. To exclude any prestimulus and post-response signals (e.g., related to the presentation of the auditory feedback tone) from spilling over into the pupil signal of interest, the time-window in which the rmANOVA was performed was restricted from the mean stimulus onset (-610ms from response, equals mean RT by definition) to the response time.

A similar hierarchical Bayesian SDT analysis as above was performed to quantify the linear relation between tonic and phasic pupil-linked arousal and decision bias (also in interaction with task), but with these pupil measurements being continuous regressors instead of drug condition. Before sampling the model, tonic and phasic pupil-linked arousal were z-scored within each participant, session, task, and block.

Drift diffusion modeling

A DDM was constructed to gain insight into which parameters of the decision process were modulated by task and phasic pupil bin[56]. The DDM was fit as a hierarchical Bayesian stimulus-coded regression model to RT distributions of "yes" and "no" response trials, using the HDDM Python package[65]. In this regression model, drift rate, non-decision time, decision boundary separation, starting point and drift criterion were allowed to vary with task, phasic pupil bin and their interaction. Model regressors were effect-coded as −1 for the liberal task and 1 for the conservative task, and −2 to 2 for the phasic pupil bins. The effects of this model can be interpreted similarly to effects derived from an ANOVA. A single chain with a length of 10,000 samples and an additional 2000 samples for burn-in was used for sampling.

Evoked response potential (ERP) neural analyses

To calculate the CPP component, single-trial response-locked data from an a-priori spatial ROI (CP1, CP2, CPz) covering centroparietal regions[23,33,63] were normalized by subtracting the average baseline activity −80 ms to 0 ms before stimulus onset and then averaged across EEG channels. Next, CPP traces were averaged within participant, drug, task, stimulus, response, and RT bin (median split). Finally, these ERP traces were averaged across drug sessions. The slope of the CPP was estimated by fitting a linear regression to the neural data in the 200 ms preceding the behavioral response. Slopes were compared with paired sample t tests (for RT bins) and with a 2 × 2 (stimulus × response) rmANOVA.

TF neural analyses

Before calculating TF representations, raw stimulus-locked and response-locked epochs were first balanced with regard to the behavioral response on the previous trial, within each task, to prevent spillover effects from the previous trials. For example, during the liberal task, participants provided more "yes" answers and prestimulus activity on a given trial may thus be driven by the disproportional amount of "yes" answers on the previous trials. After balancing epoch counts, epochs were averaged for each subject, task, stimulus, response, and phasic pupil bin. Then, these traces were averaged over stimulus, resulting in traces of neural activity exclusively related to the "yes" vs. "no" decision, but now also for each phasic pupil bin. TF representations were calculated for cropped stimulus-locked (−1000 ms to 1000 ms) and response-locked traces (−1000 ms to 250 ms). TF power was obtained through the convolution of Morlet wavelets with epoched data from 1 Hz to 40 Hz in steps of 1 Hz. For each frequency, the number of cycles was defined as:

$$number\ cycles(f) = \frac{f}{2} \quad (7)$$

Then, both stimulus-locked TF traces were cropped between −750 ms to 750 ms and response-locked TF traces were cropped between −750 ms to 0 ms. To investigate response-selective activity, TF activity was extracted from two symmetrical spatial ROIs (left hemisphere: C3 and CP3, right hemisphere: C4 and CP4) and averaged within ROI. Next, a lateralization index was calculated as follows:

$$lateralization\ index = \frac{(ROI_L - ROI_R)}{(ROI_L + ROI_R)} \quad (8)$$

This lateralization index could take values between −1 and 1, with a positive value indicating more TF power over the left hemisphere (associated with "yes" responses made with the right hand) than over the left hemisphere (associated with "no" responses made with the left hand). To analyze lateralized TF power, a permutation-based cluster-corrected (cluster

alpha: $p < 0.05$, permutations: 10,000) $2 \times 2 \times 5$ (task x response x phasic pupil bin) rmANOVA was performed.

Multivariate pattern analysis

A linear discriminant was trained on CSD-transformed EEG data from all 64 electrodes of the localizer task to distinguish Gabor-present versus Gabor-absent trials. The classifier was trained on every time point and then tested on all time-points including the one it was trained on[77]. First, a 10-fold within-localizer decoding analysis was performed on data from each experimental session to investigate whether Gabor presence was represented in neural data of the localizer task to begin with. Classifier performance of the within-localizer analyses was determined by assessing AUC. Second, we used a cross-task decoding analysis, in which we trained the classifier on the independent localizer data and tested it on data from the detection task. To increase training power, we pooled localizer data across all three drug sessions to form a single training set. Trial counts in the training set were balanced in terms of current trial target presence and target absence. Moreover, for target presence trials, trial counts were balanced for Gabor orientation and tilt offset. The performance of the classifier was assessed by extracting the amount of hits (i.e., predicted stimulus present, actual stimulus present), false alarms, misses, and correct rejections, and then calculating classifier d' and criterion similar to our behavioral analyses. Classifier criterion and d' scores were averaged across drug sessions before testing for task effects with paired sample cluster-corrected permutation t tests (two-sided, 10,000 permutations, cluster-threshold: $p < 0.05$).

Reporting summary

Further information on research design is available in the Nature Portfolio Reporting Summary linked to this article.

Data availability

All raw data (DOI: 10.21942/uva.31297489) and figure source data (DOI: 10.21942/uva.31305934) are freely available at FigShare.

Code availability

All analysis scripts are freely available at FigShare (DOI: 10.21942/uva.31305955).

Received: 18 April 2025; Accepted: 19 February 2026;
Published online: 09 March 2026

References

1. Beck, J. M., Ma, W. J., Pitkow, X. & Latham, P. E. & Pouget, A. Not noisy, just wrong: the role of suboptimal inference in behavioral variability. *Neuron* **74**, 30–39 (2012).
2. Wyart, V. & Koechlin, E. Choice variability and suboptimality in uncertain environments. *Curr. Opin. Behav. Sci.* **11**, 109–115 (2016).
3. Greene, A. S., Horien, C., Barson, D., Scheinost, D. & Constable, R. T. Why is everyone talking about brain state?. *Trends Neurosci.* **46**, 508–524 (2023).
4. McCormick, D. A., Nestvogel, D. B. & He, B. J. Neuromodulation of brain state and behavior. *Annu. Rev. Neurosci.* **43**, 391–415 (2020).
5. Waschke, L., Kloosterman, N. A., Obleser, J. & Garrett, D. D. Behavior needs neural variability. *Neuron* **109**, 751–766 (2021).
6. Jacob, S. N. & Nienborg, H. Monoaminergic neuromodulation of sensory processing. *Front. Neural Circuits* **12**, 51 (2018).
7. Lee, S.-H. & Dan, Y. Neuromodulation of brain states. *Neuron* **76**, 209–222 (2012).
8. McCormick, D. A. Cholinergic and noradrenergic modulation of thalamocortical processing. *Trends Neurosci.* **12**, 215–221 (1989).
9. Jones, B. E. Arousal systems. *Front. Biosci.* **8**, s438–s451 (2003).
10. Aston-Jones, G., Rajkowski, J., Kubiak, P. & Alexinsky, T. Locus coeruleus neurons in monkey are selectively activated by attended cues in a vigilance task. *J. Neurosci.* **14**, 4467–4480 (1994).
11. Clayton, E. C., Rajkowski, J., Cohen, J. D. & Aston-Jones, G. Phasic activation of monkey locus ceruleus neurons by simple decisions in a forced-choice task. *J. Neurosci.* **24**, 9914–9920 (2004).
12. Jones, B. E. Activity, modulation and role of basal forebrain cholinergic neurons innervating the cerebral cortex. *Prog. Brain Res.* **145**, 157–169 (2004).
13. Parikh, V., Kozak, R., Martinez, V. & Sarter, M. Prefrontal acetylcholine release controls cue detection on multiple timescales. *Neuron* **56**, 141–154 (2007).
14. Rajkowski, J., Kubiak, P., Ivanova, S. & Aston-Jones, G. State-related activity, reactivity of locus ceruleus neurons in behaving monkeys. *Adv. Pharmacol.* **42**, 740–744 (1997).
15. Devilbiss, D. M. & Waterhouse, B. D. The effects of tonic locus ceruleus output on sensory-evoked responses of ventral posterior medial thalamic and barrel field cortical neurons in the awake rat. *J. Neurosci.* **24**, 10773–10785 (2004).
16. Kalwani, R. M., Joshi, S. & Gold, J. I. Phasic activation of individual neurons in the locus ceruleus/subceruleus complex of monkeys reflects rewarded decisions to go but not stop. *J. Neurosci.* **34**, 13656–13669 (2014).
17. Aston-Jones, G. & Cohen, J. D. An integrative theory of locus coereleus-norepinephrine function: adaptive gain and optimal performance. *Annu. Rev. Neurosci*. **28**, 403–450 (2005).
18. de Gee, J. W. et al. Dynamic modulation of decision biases by brainstem arousal systems. *eLife* **6**, e23232 (2017).
19. Joshi, S., Li, Y., Kalwani, R. M. & Gold, J. I. Relationships between pupil diameter and neuronal activity in the locus coeruleus, colliculi, and cingulate cortex. *Neuron* **89**, 221–234 (2016).
20. Reimer, J. et al. Pupil fluctuations track rapid changes in adrenergic and cholinergic activity in cortex. *Nat. Commun.* **7**, 13289 (2016).
21. Beerendonk, L. et al. A disinhibitory circuit mechanism explains a general principle of peak performance during mid-level arousal. *Proc. Natl. Acad. Sci.* **121**, e2312898121 (2024).
22. McGinley, M. J., David, S. V. & McCormick, D. A. Cortical membrane potential signature of optimal states for sensory signal detection. *Neuron* **87**, 179–192 (2015).
23. Nuiten, S. A., Gee, J. W. de, Zantvoord, J. B., Fahrenfort, J. J. & Gaal, S. van. Pharmacological elevation of catecholamine levels improves perceptual decisions, but not metacognitive insight. *eNeuro* **11**, ENEURO.0019-24.2024 (2024).
24. Podvalny, E., King, L. E. & He, B. J. Spectral signature and behavioral consequence of spontaneous shifts of pupil-linked arousal in human. *eLife* **10**, e68265 (2021).
25. de Gee, J. W., Knapen, T. & Donner, T. H. Decision-related pupil dilation reflects upcoming choice and individual bias. *Proc. Natl. Acad. Sci.* **111**, E618–E625 (2014).
26. de Gee, J. W. et al. Pupil-linked phasic arousal predicts a reduction of choice bias across species and decision domains. *eLife* **9**, e54014 (2020).
27. Urai, A. E., Braun, A. & Donner, T. H. Pupil-linked arousal is driven by decision uncertainty and alters serial choice bias. *Nat. Commun.* **8**, 14637 (2017).
28. Hebisch, J. et al. Task-irrelevant stimuli reliably boost phasic pupil-linked arousal but do not affect decision formation. *Sci. Rep.* **14**, 28380 (2024).
29. Lewandowska, K., Gągol, A., Sikora-Wachowicz, B., Marek, T. & Fąfrowicz, M. Saying "yes" when you want to say "no" - pupil dilation reflects evidence accumulation in a visual working memory recognition task. *Int. J. Psychophysiol.* **139**, 18–32 (2019).
30. Schriver, B. J., Perkins, S. M., Sajda, P. & Wang, Q. Interplay between components of pupil-linked phasic arousal and its role in driving behavioral choice in Go/No-Go perceptual decision-making. *Psychophysiology* **57**, e13565 (2020).
31. De Gee, J. W. et al. Strategic stabilization of arousal boosts sustained attention. *Curr. Biol.* **34**, 4114–4128.e6 (2024).

32. Gelbard-Sagiv, H., Magidov, E., Sharon, H., Hendler, T. & Nir, Y. Noradrenaline modulates visual perception and late visually evoked activity. *Curr. Biol.* **28**, 2239–2249.e6 (2018).
33. Nuiten, S. A., De Gee, J. W., Fahrenfort, J. J. & van Gaal, S. Catecholaminergic neuromodulation and selective attention jointly shape perceptual decision making. *eLife* **12**, RP87022 (2023).
34. Hasselmo, M. E. The role of acetylcholine in learning and memory. *Curr. Opin. Neurobiol.* **16**, 710–715 (2006).
35. Hasselmo, M. E. & Sarter, M. Modes and models of forebrain cholinergic neuromodulation of cognition. *Neuropsychopharmacology* **36**, 52–73 (2011).
36. Yu, A. J. & Dayan, P. *Acetylcholine, Norepinephrine, and Spatial Attention*. https://papers.ssrn.com/abstract=2978391 (2003).
37. Yu, A. J. & Dayan, P. Uncertainty, neuromodulation, and attention. *Neuron* **46**, 681–692 (2005).
38. Shine, J. M. Neuromodulatory influences on integration and segregation in the brain. *Trends Cogn. Sci.* **23**, 572–583 (2019).
39. Ratcliff, R., Smith, P. L., Brown, S. D. & McKoon, G. Diffusion decision model: current issues and history. *Trends Cogn. Sci.* **20**, 260–281 (2016).
40. DeCarlo, L. T. Signal detection theory and generalized linear models. *Psychol. Methods* **3**, 186–205 (1998).
41. Green, D. M. & Swets, J. A. *Signal Detection Theory and Psychophysics*. xi, 455 (John Wiley, Oxford, England, 1966).
42. Gelman, A., Carlin, J. B., Stern, H. S. & Rubin, D. B. *Bayesian Data Analysis*. (Chapman and Hall/CRC, 1995).
43. Kruschke, J. K. *Doing Bayesian Data Analysis: A Tutorial with R, JAGS, and Stan*. (Academic Press, Waltham MA, 2015).
44. Makowski, D., Ben-Shachar, M. S., Chen, S. H. A. & Lüdecke, D. Indices of effect existence and significance in the Bayesianframework. *Front. Psychol*. **10**, 2767 (2019).
45. Kloosterman, N. A. et al. Humans strategically shift decision bias by flexibly adjusting sensory evidence accumulation. *eLife* **8**, e37321 (2019).
46. Mathôt, S. & Vilotijević, A. Methods in cognitive pupillometry: design, preprocessing, and statistical analysis. *Behav. Res. Methods* **55**, 3055–3077 (2023).
47. Mathôt, S., Dalmaijer, E. & Grainger, J. & Van der Stigchel, S. The pupillary light response reflects exogenous attention and inhibition of return. *J. Vis.* **14**, 7 (2014).
48. Wang, C.-A. & Munoz, D. P. Modulation of stimulus contrast on the human pupil orienting response. *Eur. J. Neurosci.* **40**, 2822–2832 (2014).
49. Wierda, S. M., van Rijn, H., Taatgen, N. A. & Martens, S. Pupil dilation deconvolution reveals the dynamics of attention at high temporal resolution. *Proc. Natl. Acad. Sci.* **109**, 8456–8460 (2012).
50. Zylberberg, A., Oliva, M. & Sigman, M. Pupil dilation: a fingerprint of temporal selection during the "attentional blink". *Front. Psychol.* **3**, 316 (2012).
51. Beerendonk, L. et al. Adaptive arousal regulation: Pharmacologically shifting the peak of the Yerkes–Dodson curve by catecholaminergic enhancement of arousal. *Proc. Natl. Acad. Sci.* **122**, e2419733122 (2025).
52. Knapen, T. et al. Cognitive and ocular factors jointly determine pupil responses under equiluminance. *PLoS One* **11**, e0155574 (2016).
53. Mridha, Z. et al. Graded recruitment of pupil-linked neuromodulation by parametric stimulation of the vagus nerve. *Nat. Commun.* **12**, 1539 (2021).
54. Gold, J. I. & Shadlen, M. N. The neural basis of decision making. *Annu. Rev. Neurosci.* **30**, 535–574 (2007).
55. Shadlen, M. N. & Kiani, R. Decision making as a window on cognition. *Neuron* **80**, 791–806 (2013).
56. Ratcliff, R. & McKoon, G. The diffusion decision model: theory and data for two-choice decision tasks. *Neural Comput.* **20**, 873–922 (2008).
57. Kelly, S. P. & O'Connell, R. G. Internal and external influences on the rate of sensory evidence accumulation in the human brain. *J. Neurosci.* **33**, 19434–19441 (2013).
58. Kiani, R., Hanks, T. D. & Shadlen, M. N. Bounded integration in parietal cortex underlies decisions even when viewing duration is dictated by the environment. *J. Neurosci.* **28**, 3017–3029 (2008).
59. Pereira, M. et al. Evidence accumulation relates to perceptual consciousness and monitoring. *Nat. Commun.* **12**, 3261 (2021).
60. Ratcliff, R. A diffusion model account of response time and accuracy in a brightness discrimination task: Fitting real data and failing to fit fake but plausible data. *Psychon. Bull. Rev.* **9**, 278–291 (2002).
61. Tagliabue, C. F. et al. The EEG signature of sensory evidence accumulation during decision formation closely tracks subjective perceptual experience. *Sci. Rep.* **9**, 4949 (2019).
62. Stine, G. M., Zylberberg, A., Ditterich, J. & Shadlen, M. N. Differentiating between integration and non-integration strategies in perceptual decision making. *eLife* **9**, e55365 (2020).
63. O'Connell, R. G., Dockree, P. M. & Kelly, S. P. A supramodal accumulation-to-bound signal that determines perceptual decisions in humans. *Nat. Neurosci.* **15**, 1729–1735 (2012).
64. O'Connell, R. G. & Kelly, S. P. Neurophysiology of human perceptual decision-making. *Annu. Rev. Neurosci.* **44**, 495–516 (2021).
65. Wiecki, T., Sofer, I. & Frank, M. HDDM: hierarchical bayesian estimation of the drift-diffusion model in python. *Front. Neuroinformatics* **7**, 55610 (2013).
66. de Lange, F. P., Rahnev, D. A., Donner, T. H. & Lau, H. Prestimulus oscillatory activity over motor cortex reflects perceptual expectations. *J. Neurosci.* **33**, 1400–1410 (2013).
67. Donner, T. H., Siegel, M., Fries, P. & Engel, A. K. Buildup of choice-predictive activity in human motor cortex during perceptual decision making. *Curr. Biol.* **19**, 1581–1585 (2009).
68. Popovych, S. et al. Movement-related phase locking in the delta–theta frequency band. *NeuroImage* **139**, 439–449 (2016).
69. Urbano, A., Babiloni, C., Onorati, P. & Babiloni, F. Dynamic functional coupling of high resolution EEG potentials related to unilateral internally triggered one-digit movements. *Electroencephalogr. Clin. Neurophysiol.* **106**, 477–487 (1998).
70. Wilming, N., Murphy, P. R., Meyniel, F. & Donner, T. H. Large-scale dynamics of perceptual decision information across human cortex. *Nat. Commun.* **11**, 5109 (2020).
71. Wyart, V., de Gardelle, V., Scholl, J. & Summerfield, C. Rhythmic fluctuations in evidence accumulation during decision making in the human brain. *J. Vis.* **12**, 1113 (2012).
72. Hamel-Thibault, A., Thénault, F., Whittingstall, K. & Bernier, P.-M. Delta-band oscillations in motor regions predict hand selection for reaching. *Cereb. Cortex* **28**, 574–584 (2018).
73. Kelly, S. P., Corbett, E. A. & O'Connell, R. G. Neurocomputational mechanisms of prior-informed perceptual decision-making in humans. *Nat. Hum. Behav.* **5**, 467–481 (2021).
74. Kirschner, H., Fischer, A. G., Danielmeier, C., Klein, T. A. & Ullsperger, M. Cortical β power reflects a neural implementation of decision boundary collapse in speeded decisions. *J. Neurosci*. **44**, e0534232023 (2024).
75. Murphy, P. R., Boonstra, E. & Nieuwenhuis, S. Global gain modulation generates time-dependent urgency during perceptual choice in humans. *Nat. Commun.* **7**, 13526 (2016).
76. Steinemann, N. A., O'Connell, R. G. & Kelly, S. P. Decisions are expedited through multiple neural adjustments spanning the sensorimotor hierarchy. *Nat. Commun.* **9**, 3627 (2018).
77. King, J.-R. & Dehaene, S. Characterizing the dynamics of mental representations: the temporal generalization method. *Trends Cogn. Sci.* **18**, 203–210 (2014).
78. Fahrenfort, J. J., Johnson, P. A., Kloosterman, N. A., Stein, T. & Gaal, S. van. Criterion placement threatens the construct validity of neural measures of consciousness. *eLife* **13**, RP95663 (2025).

79. Devilbiss, D. M., Page, M. E. & Waterhouse, B. D. Locus Ceruleus Regulates Sensory Encoding By Neurons And Networks In Waking Animals. *J. Neurosci.* **26**, 9860 (2006).
80. McGinley, M. J. et al. Waking state: rapid variations modulate neural and behavioral responses. *Neuron* **87**, 1143–1161 (2015).
81. Schriver, B. J., Bagdasarov, S. & Wang, Q. Pupil-linked arousal modulates behavior in rats performing a whisker deflection direction discrimination task. *J. Neurophysiol.* **120**, 1655 (2018).
82. Waschke, L., Tune, S. & Obleser, J. Local cortical desynchronization and pupil-linked arousal differentially shape brain states for optimal sensory performance. *eLife* **8**, e51501 (2019).
83. Gritton, H. J. et al. Cortical cholinergic signaling controls the detection of cues. *Proc. Natl. Acad. Sci.* **113**, E1089–E1097 (2016).
84. Dahl, M. J., Mather, M. & Werkle-Bergner, M. Noradrenergic modulation of rhythmic neural activity shapes selective attention. *Trends Cogn. Sci.* **26**, 38–52 (2022).
85. Iemi, L., Chaumon, M., Crouzet, S. M. & Busch, N. A. Spontaneous neural oscillations bias perception by modulating baseline excitability. *J. Neurosci.* **37**, 807–819 (2017).
86. Bouret, S. & Sara, S. J. Reward expectation, orientation of attention and locus coeruleus-medial frontal cortex interplay during learning. *Eur. J. Neurosci.* **20**, 791–802 (2004).
87. Krishnamurthy, K., Nassar, M. R., Sarode, S. & Gold, J. I. Arousal-related adjustments of perceptual biases optimize perception in dynamic environments. *Nat. Hum. Behav.* **1**, 0107 (2017).
88. Nassar, M. R. Toward a computational role for locus coeruleus/norepinephrine arousal systems. *Curr. Opin. Behav. Sci.* **59**, 101407 (2024).
89. Nassar, M. R. et al. Rational regulation of learning dynamics by pupil-linked arousal systems. *Nat. Neurosci.* **15**, 1040–1046 (2012).
90. Yu, A. J. & Cohen, J. D. Sequential effects: superstition or rational behavior? in *Advances in Neural Information Processing Systems* **21**, 1873–1880 (Curran Associates, Inc., 2008).
91. Frömer, R., Nassar, M. R., Ehinger, B. V. & Shenhav, A. Common neural choice signals can emerge artefactually amid multiple distinct value signals. *Nat. Hum. Behav.* **8**, 2194–2208 (2024).
92. O'Connell, R. G., Parés-Pujolràs, E., Corbett, E. A., Feuerriegel, D. & Kelly, S. P. Regressing away common neural choice signals does not make them artifacts: comment on Frömer et al. 2024. *Imaging Neurosci.* **3**, IMAG.a.60 (2025).
93. Keitel, A. & Gross, J. Individual human brain areas can be identified from their characteristic spectral activation fingerprints. *PLoS Biol.* **14**, e1002498 (2016).
94. Urai, A. E. & Donner, T. H. Persistent activity in human parietal cortex mediates perceptual choice repetition bias. *Nat. Commun.* **13**, 6015 (2022).
95. Saleh, M., Reimer, J., Penn, R., Ojakangas, C. L. & Hatsopoulos, N. G. Fast and slow oscillations in human primary motor cortex predict oncoming behaviorally relevant cues. *Neuron* **65**, 461–471 (2010).
96. Mathôt, S. Pupillometry: psychology, physiology, and function. *Peer J.* **6**, e4422 (2018).
97. Ludwig, M., Wienke, C., Betts, M. J., Zaehle, T. & Hämmerer, D. Current challenges in reliably targeting the noradrenergic locus coeruleus using transcutaneous auricular vagus nerve stimulation (taVNS). *Auton. Neurosci.* **236**, 102900 (2021).
98. Sharon, O., Fahoum, F. & Nir, Y. Transcutaneous vagus nerve stimulation in humans induces pupil dilation and attenuates alpha oscillations. *J. Neurosci.* **41**, 320–330 (2021).
99. Skora, L., Marzecová, A. & Jocham, G. Tonic and phasic transcutaneous auricular vagus nerve stimulation (taVNS) both evoke rapid and transient pupil dilation. *Brain Stimul.* **17**, 233–244 (2024).
100. Tona, K.-D., Murphy, Peter, R., Brown, S. B. R. E. & Nieuwenhuis, S. The accessory stimulus effect is mediated by phasic arousal: a pupillometry study: phasic arousal and the AS effect. *Psychophysiology* **53**, 1108–1113 (2016).
101. Pfeffer, T. et al. Catecholamines alter the intrinsic variability of cortical population activity and perception. *PLOS Biol.* **16**, e2003453 (2018).
102. Pfeffer, T. et al. Coupling of pupil- and neuronal population dynamics reveals diverse influences of arousal on cortical processing. *eLife* https://elifesciences.org/articles/71890/figures (2022)
103. Silver, M. A., Shenhav, A. & D'Esposito, M. Cholinergic enhancement reduces spatial spread of visual responses in human early visual cortex. *Neuron* **60**, 904–914 (2008).
104. Sarter, M. & Lustig, C. Forebrain cholinergic signaling: wired and phasic, not tonic, and causing behavior. *J. Neurosci.* **40**, 712–719 (2020).
105. Xu, Y. et al. Effects of alertness on perceptual detection and discrimination. *Cortex* **190**, 262–285 (2025).
106. King, J.-R. & Dehaene, S. A model of subjective report and objective discrimination as categorical decisions in a vast representational space. *Philos. Trans. R. Soc. B Biol. Sci.* https://doi.org/10.1098/rstb.2013.0204 (2014).
107. Mazor, M., Maimon-Mor, R. O., Charles, L. & Fleming, S. M. Paradoxical evidence weighting in confidence judgments for detection and discrimination. *Atten. Percept. Psychophys.* https://doi.org/10.3758/s13414-023-02710-8 (2023).
108. Simpson, D. & Plosker, G. L. Atomoxetine: a review of its use in adults with attention deficit hyperactivity disorder. *Drugs* **64**, 205–222 (2004).
109. Rogers, S. L. & Friedhoff, L. T. Pharmacokinetic and pharmacodynamic profile of donepezil HCl following single oral doses. *Br. J. Clin. Pharmacol.* **46**, 1–6 (1998).
110. Bond, A. & Lader, M. The use of analogue scales in rating subjective feelings. *Br. J. Med. Psychol.* **47**, 211–218 (1974).
111. Peirce, J. W. PsychoPy—psychophysics software in Python. *J. Neurosci. Methods* **162**, 8–13 (2007).
112. Kaernbach, C. Simple adaptive testing with the weighted up-down method. *Percept. Psychophys.* **49**, 227–229 (1991).
113. Gramfort, A. et al. MEG and EEG data analysis with MNE-Python. *Front. Neurosci.* **7**, 267 (2013).
114. Jas, M., Engemann, D. A., Bekhti, Y., Raimondo, F. & Gramfort, A. Autoreject: automated artifact rejection for MEG and EEG data. *NeuroImage* **159**, 417–429 (2017).
115. JASP TEAM. JASP (Version 0.95.0)[Computer software]. (2025).
116. Jarosz, A. F. & Wiley, J. What are the odds? A practical guide to computing and reporting bayes factors. *J. Probl. Solving* **7**, 2 (2014).
117. Abril-Pla, O. et al. PyMC: a modern, and comprehensive probabilistic programming framework in Python. *PeerJ Comput. Sci.* **9**, e1516 (2023).
118. Gelman, A. & Rubin, D. B. Inference from iterative simulation using multiple sequences. *Stat. Sci.* **7**, 457–472 (1992).

Acknowledgements

This work was supported by the European Research Council (ERC Starting Grant 715605, awarded to Simon van Gaal) under the Horizon Europe program.

Author contributions

S.A.N., J.J.F., and S.v.G. designed research; S.A.N. and J.Z. performed research; S.A.N. and J.W.d.G. analyzed data; S.v.G. supervised the project; S.A.N. and S.v.G. wrote the paper; J.W.d.G., J.J.F., and P.S. edited the manuscript.

Competing interests

The authors declare no competing interests.

Additional information

Supplementary information The online version contains supplementary material available at https://doi.org/10.1038/s42003-026-09776-8.

Correspondence and requests for materials should be addressed to Stijn Adriaan Nuiten or Simon van Gaal.

Peer review information *Communications Biology* thanks Julian Q. Kosciessa and the other, anonymous, reviewer(s) for their contribution to the peer review of this work. Primary Handling Editors: Jacqueline Gottlieb and Benjamin Bessieres. [A peer review file is available].